TECHNICAL NOTE

D-26

MOVING-COCKPIT SIMULATOR INVESTIGATION OF THE MINIMUM TOLERABLE LONGITUDINAL MANEUVERING STABILITY

By B. Porter Brown and Harold I. Johnson

Langley Research Center
Langley Field, Va.

NATIONAL AERONAUTICS AND SPACE ADMINISTRATION

WASHINGTON September 1959

NATIONAL AERONAUTICS AND SPACE ADMINISTRATION

TECHNICAL NOTE D-26

MOVING-COCKPIT SIMULATOR INVESTIGATION OF THE MINIMUM TOLERABLE LONGITUDINAL MANEUVERING STABILITY

By B. Porter Brown and Harold I. Johnson

SUMMARY

Tests have been made on the NASA normal acceleration and pitch (NAP) simulator utilizing a close-formation flying task for the purpose of studying the effects on controllability of various amounts of aircraft stability and various amounts of stick force and position gradients. The simulator represents only the cockpit portion of an aircraft or space vehicle and it is able to rotate in pitch and to move vertically. The motions provided by the simulator are those associated with the short-period longitudinal mode.

The results from these tests indicate that the maneuver neutral point is a reasonable rearward limit for the aircraft center of gravity with respect to controllability. Beyond this point control is extremely uncertain. The best performances in the simulated formation-flying task were obtained with force gradients many times larger than those specified for gross maneuvering for fighter-type airplanes in present-day flying-qualities requirements. This result indicates the importance of force gradient to precision control. These forces would, however, be excessive for maneuvers requiring steady accelerations except when the center of gravity is at or very near to the maneuver point. For the cases with some amount of stick force gradient, performance improved when the stick position gradient was increased from 1.13° to 2.0° of stick rotation per degree of tail deflection. A further increase to 4.5° showed no improvement for these cases. For the cases with zero forces, each increase in position gradient resulted in increased performance. The pilots felt, however, that the effect of position gradient was small. Reduction in aircraft damping resulted in somewhat lower performance; however, this effect was not considered to be serious in this investigation. The differences in performance as measured with and without the pitching motion were very small for one pilot and negligible for the other. Therefore, the pitching-motion cues were not considered to be of importance to performance in close-formation flying.

INTRODUCTION

The National Aeronautics and Space Administration has built a simulator for the purpose of studying piloting problems associated with longitudinal control of aircraft and space vehicles. The simulator represents only the cockpit portion of the aircraft or space vehicle and it is able to rotate in pitch and to move vertically. The motions provided by the simulator are those associated with the short-period longitudinal mode. These motions of the simulator subject the pilot's body to the proper forces such that the pilot is provided with the "feeling" of actual flight, a feature that heretofore has been lacking in nearly all flight simulation investigations. This facility, which is referred to as the NAP chair (from the words normal acceleration and pitch), is located at the Langley Research Center. A complete description of the simulator is given in a later section of this paper.

Part of the test program undertaken with this equipment consisted of a study to determine the *minimum* tolerable maneuvering stability. The minimum tolerable maneuvering stability is important for at least two reasons. First, for conventionally controlled airplanes there is a trim drag penalty at low supersonic speeds arising from excessive longitudinal stability and this degree of excessive stability and the resulting extra drag are associated directly with the minimum stability that can be tolerated and that usually occurs at some lower speed. Second, for airplanes normally flying with stability-augmentation equipment, it is desirable to start with approximately zero maneuver margin of the basic airframe; however, in case of failure of the automatic stabilization equipment, it is imperative to know the minimum stability that the human pilot can tolerate in order to prevent loss of equipment and possible loss of human life.

The simulator was made to possess dynamic characteristics typical of a present-day fighter flying at high speeds and low altitude with maneuver margins ranging from highly stable to unstable of enough magnitude to prevent successful flight by a human pilot. At each set of period and damping characteristics tested, the apparent stick-fixed and stick-free stability, represented by the stick travel per g and the stick force per g, respectively, were varied in order to determine the effects of these parameters on the pilot performances. Although some attention was given to pilot opinions, the primary emphasis has been placed on the quantitative performances scored by the pilots while carrying out a fixed and predictable - yet exacting - task simulating close-formation flying.

SYMBOLS

A_n	normal acceleration
C_{L_α}	rate of change of aircraft lift coefficient with angle of attack
C_{L_δ}	rate of change of aircraft lift coefficient with tail deflection
$C_{L_{D\alpha}}$	rate of change of aircraft lift coefficient with nondimensional rate of change of angle of attack
$C_{L_{D\theta}}$	rate of change of aircraft lift coefficient with nondimensional rate of change of pitch angle
C_{m_α}	rate of change of aircraft pitching-moment coefficient with angle of attack
C_{m_δ}	rate of change of aircraft pitching-moment coefficient with tail deflection
$C_{m_{D\alpha}}$	rate of change of aircraft pitching-moment coefficient with nondimensional rate of change of angle of attack
$C_{m_{D\theta}}$	rate of change of aircraft pitching-moment coefficient with nondimensional rate of change of pitch angle
$\bar{c}$	wing mean aerodynamic chord
D	differential operator
d	distance from pilot's eyes to target
F_s	stick force
g	acceleration due to gravity
h	altitude or vertical position of cockpit
$\dot{h}$	vertical velocity of cockpit
$\ddot{h}$	vertical acceleration of cockpit, A_n
h_b	height of ball from floor

h_s	height of sighting image from floor
$h_{s_{An}}$	height of sighting image from floor with chair at zero pitch angle
$\Delta h_{s,\theta}$	change in height of sighting image due to pitch angle
I_c	control-system inertia
I_Y	aircraft moment of inertia about Y-axis
$\frac{K_{1,\alpha}}{D}$	output of first-stage servo and input of second servo in altitude circuit, $\dot{h}$
$\frac{K_{2,\alpha}}{D^2}$	output of second-stage servo in altitude circuit, h
K_Y	radius of gyration about aircraft Y-axis
M	Mach number
m	aircraft mass
S	aircraft wing area
V	airspeed
$V_{\epsilon,\alpha,1}$	input voltage of first-stage servo in altitude circuit ($\approx \ddot{h}$)
$V_{\epsilon,\alpha,2}$	input voltage of angle-of-attack servo
α	angle of attack
α_D	angular displacement of α-simulator from trim
γ	flight-path angle
δ_s	stick position
δ_T	longitudinal control-surface position
δ_s/δ_T	control-system gearing constant

ϵ_h error between height of ball and height of sighting image

θ cockpit pitch angle, $\alpha + \gamma$

$\ddot{\theta}$ pitching acceleration

μ aircraft relative-density factor, $m/\rho S\bar{c}$

ρ air density

DESCRIPTION OF APPARATUS

Simulator

An overall view of the simulator is shown in figure 1. Figure 2 shows a schematic drawing of the simulator. The pilot's objective during the tests was to make the sighting image coincident with the target as shown in figures 1 and 2. Figure 3 shows a block diagram of the simulator. Many of the important components shown in the diagram are shown in detail in subsequent figures.

A control stick is mounted in the cockpit of the simulator as shown in figure 4. A spring connected to the control stick supplies the control forces. The inertia of the control system is about 0.3 slug-feet^2. Also connected to the stick is a synchrogenerator. Motions of the stick are transmitted electrically through this generator to a synchromotor mounted on a stationary platform outside of the cockpit. (See fig. 5.) An aluminum disk mounted on the movable shaft of the synchromotor represents the inertia of the simulated aircraft. Simulated aircraft damping is applied to this mass by means of an electrical eddy-current damper. Increasing the voltage on the damper increases the damping of the simulated airplane. The spring restoring moment representing angle-of-attack stability is provided in this system by means of the voltage impressed on the field coils of the synchrogenerator and synchromotor. This spring-mass-dashpot system, which represents the dynamics of the aircraft, is referred to hereinafter as the "α-simulator." Also included in the α-simulator are two additional coils which supply a destabilizing spring force on the shaft of the synchromotor. This function is accomplished by use of a curved slug entering one or the other of a pair of solenoids. These coils and the slug are also shown in figure 5. This destabilizing force is proportional to the voltage across the destabilizing coils in such a way that increasing this voltage produces an effect on the simulator dynamics which is very similar to that obtained by moving the center of gravity of an aircraft to a more rearward position. When the destabilizing voltage is increased to the point that the destabilizing

force at any given disk deflection is exactly equal to the stabilizing force produced by the generator-motor field voltage, the system is neutrally stable. This condition represents an aircraft the center of gravity of which is located on the maneuver point. Maneuvering instability (negative maneuver margin) can be simulated by making the destabilizing force gradient larger than the stabilizing force gradient. The angular position of the disk away from trim represents the angle of attack of the simulated aircraft. The disk position is sensed by two miniature synchrogenerators connected to the ends of the rotor shaft of the synchromotor. Signals from these miniature generators are amplified and are used to control the pitch angle and the normal acceleration of the cockpit simultaneously.

Pitch circuit.- The pitch circuit is actually divided into two phases, one representing angle of attack α and the other representing flight-path angle γ. The sum of these two angles is equal to the total pitch angle of the cockpit. The pitch circuit is very similar to that described in reference 1. The pitching motion representing angle-of-attack change is provided by a positioning servo which follows the motion of the α-simulator and drives one of two hydraulic actuators that are connected to the cockpit through an adding linkage. (See fig. 6.) The output of this angle-of-attack servo is sensed and used as the input to an integrating servo which supplies fluid to the other hydraulic actuator and which provides another pitching motion which is proportional to rate of change of the flight-path angle. It should be noted that the positioning servo in the angle-of-attack circuit provides a distinct static relationship between stick angle and airplane angle of attack whereas the integrating servo in the flight-path circuit provides a rate of rotation (rate of change of flight-path angle) dependent upon the magnitude of the angle of attack. The maximum cockpit rotation due to the angle-of-attack actuator is about $\pm 4^{\circ}$. Larger angles, however, might be reached through the ensuing action of the flight-path-angle actuator.

Altitude circuit.- The primary electrical input for the altitude circuit, which also originates from the α-simulator, is fed into two integrating servos in series. (Refer to fig. 3.) As mentioned in the previous section this primary signal is proportional to angle of attack and therefore is also proportional to normal acceleration (unsteady lift effects being neglected). Double integration of the normal-acceleration signal produces altitude or vertical displacement of the cockpit. The second integrating servo in this circuit is a 40-horsepower hydraulic unit for which a detailed description can be found in reference 2. The output of this unit rotates a pulley and continuous cable system. The cockpit constitutes an integral link of this continuous cable system. This output (or driving end), the lower pulley, and the continuous cable are shown in figure 7. Maximum usable vertical travel of the cockpit is 8 feet. The maximum increment of acceleration obtainable is about ± 1g.

This acceleration limit results from power limitations of the first integrating servo in the altitude circuit. This amount of acceleration was found to be sufficiently high for this investigation. The static weight of the cockpit is counterbalanced by a set of eight bungee chords supported from a point approximately 65 feet above the floor.

Target and sighting system.- A projector, mounted to the side of the cockpit on a level with the pilot's eyes (fig. 4), projects a sighting image in the form of a cross on a screen located approximately 7 feet in front of the pilot's eyes. The screen is in the form of a section of a hollow cylinder, the axis of which is vertical and passes approximately through the pilot's eyes. The screen is painted light blue and the joints in it are concealed. When seated in the cockpit, the pilot is unable to see beyond the edges of the screen in any direction. These features represent an attempt to produce a psychological feeling of actual flight by allowing the pilot to see only the relative motion between the target and the sighting image. The target, which is a ball approximately 1 inch in diameter and located 7 feet in front of the pilot's eyes, moves up and down with a total excursion of approximately 5 feet. The target motion is adjustable and the particular motion used in these tests is discussed more fully in a later section.

Safety features.- The bungee cords, mentioned previously in connection with the mass balancing of the cockpit, also serve as a safety suspension system in the event of a failure of the main driving cable.

An automatic cut-off system is provided to prevent damage in case of control circuit failures such as a "run-away" or "hard-over signal." The cut-off system consists of mechanical linkages which feed back the vertical position of the chair and cancel the input signal to the 40-horsepower unit. This linkage is arranged in such a way that only the last 6 inches of vertical motion (beyond the usable travel) at the top and bottom actuate the linkage and cancel the input signal. Viscous dampers are attached to the cut-off linkages to prevent undesirable oscillations. For the present tests, the vertical velocity of the cockpit was limited to a maximum of 5 feet per second by mechanical stops on the output of the first servo. This velocity was found to be sufficient to perform the task required in the present tests and the pilots commented that this velocity was ample for the flight conditions being simulated. When the cockpit is traveling at its maximum velocity and encounters the automatic cut-off system, the pilot is subjected to a deceleration of about $4\frac{1}{2}g$ for a small fraction of a second. The cockpit is equipped with shoulder and lap belts and the pilot is required to wear a crash helmet. (See fig. 4.)

A duplicate control system is provided at the ground operator's control station (fig. 8) so that in the event of a failure in the pilot's

control system, the ground operator can assume complete control. Intercommunication is provided between the pilot and the ground operators for safety purposes and also as a means of obtaining immediate pilot opinion of each configuration.

Characteristics of NAP Simulator

Theoretical.- Comparisons between the nondimensionalized transfer functions of an idealized rigid airplane (ref. 3) and those of the idealized NAP simulator (no servo lags) are shown by the following expressions:

For the airplane:

$$\left|\frac{A_n}{\delta_T}\right| = \frac{V^2}{g\bar{c}} \frac{AD^2 + BD + C}{ED^2 + FD + G}$$

$$\left|\frac{\theta}{\delta_T}\right| = \frac{HD + C}{ED^3 + FD^2 + GD}$$

$$\left|\frac{\alpha}{\delta_T}\right| = \frac{-AD + K}{ED^2 + FD + G}$$

wherein

$$A = 2\mu K_y{}^2 C_{L_\delta}$$

$$B = C_{L_{D\alpha}} C_{m_\delta} - C_{L_\delta} C_{m_{D\alpha}} + C_{L_{D\theta}} C_{m_\delta} - C_{L_\delta} C_{m_{D\theta}}$$

$$C = C_{L_\alpha} C_{m_\delta} - C_{L_\delta} C_{m_\alpha}$$

$$E = 4\mu^2 K_y{}^2 + 2\mu K_y{}^2 C_{L_{D\alpha}}$$

$$F = -2\mu C_{m_{D\theta}} - C_{m_{D\theta}} C_{L_{D\alpha}} + C_{L_{D\theta}} C_{m_{D\alpha}} + 2\mu K_y{}^2 C_{L_\alpha} - 2\mu C_{m_{D\alpha}}$$

$$G = -2\mu C_{m_\alpha} + C_{L_{D\theta}} C_{m_\alpha} - C_{L_\alpha} C_{m_{D\theta}}$$

$$H = 2\mu C_{m_\delta} + C_{L_{D\alpha}} C_{m_\delta} - C_{L_\delta} C_{m_{D\alpha}}$$

$$K = 2\mu C_{m_\delta} - C_{L_{D\theta}} C_{m_\delta} + C_{L_\delta} C_{m_{D\theta}}$$

For the NAP simulator:

$$\left|\frac{A_n}{\delta_T}\right| = \frac{V^2}{g\bar{c}} \frac{C'}{E'D^2 + F'D + G'}$$

$$\left|\frac{\theta}{\delta_T}\right| = \frac{H'D + C'}{E'D^3 + F'D^2 + G'D}$$

$$\left|\frac{\alpha}{\delta_T}\right| = \frac{K'}{E'D^2 + F'D + G'}$$

wherein

$$C' = C_{L_\alpha} C_{m_\delta}$$

$$E' = 4\mu^2 K_y^2$$

$$F' = 2\mu K_y^2 C_{L_\alpha} - 2\mu C_{m_{D\alpha}}$$

$$G' = -2\mu C_{m_\alpha}$$

$$H' = 2\mu C_{m_\delta}$$

$$K' = 2\mu C_{m_\delta}$$

An examination of the foregoing transfer functions shows that the characteristic equations (denominators) of the idealized airplane and NAP simulator are of identical form. The numerators, however, are of different form in the cases of the A_n/δ_T and α/δ_T transfer functions. These differences arise from the fact that no attempt was made to include tail lift characteristics in the NAP simulator and no provision was made to represent the $C_{m_{D\theta}}$ and $C_{L_{D\theta}}$ damping terms. The latter deficiency can be partially corrected by adjusting the period and damping characteristics of the simulator to those of the simulated airplane because both have characteristic equations of identical form.

In order to determine the effect of the simplifications resorted to in the NAP simulator, a typical set of stability and control parameters

(Case II of ref. 3) were inserted into the A_n/δ_T and θ/δ_T transfer functions of both the airplane and the simulator and the resulting frequency-response curves are compared in figure 9. In evaluating the transfer functions of the simulator, the characteristic equations of the airplane were used.

Actual.- In an actual airplane the transfer functions relating control-stick deflection to airplane response are perhaps of greater interest than the idealized rigid-airplane transfer functions relating tail deflection to airplane response discussed in the foregoing section. The theoretical set of transfer functions will, in general, differ considerably from the actual set of transfer functions because of the dynamic characteristics of the power control system and the kinematic deficiencies of the control system (backlash, control-system deflection, etc.) as well as possible aeroelastic effects exhibited by the airplane.

In the NAP simulator, on the other hand, the control system is of extremely high quality; thus, the nonlinearities normally attributed to control-system deficiencies are negligible. However, the simulator has two sets of two cascaded servos which do not have altogether ideal dynamic characteristics and which also possess kinematic deficiencies and nonlinearities such as backlash and static friction. For this reason it is of interest to compare measured frequency-response characteristics of the NAP simulator with those of an actual airplane in flight. Such a comparison is made in figure 10.

Figure 10 shows the frequency response of normal acceleration to stick deflection for the simulator and a typical jet fighter airplane. No attempt was made to adjust the simulator dynamics exactly to those of the airplane; even so, the similarity in general trends is immediately evident. However, it is apparent from figure 10 that at frequencies above about 1 cycle per second the phase lags of the simulator increase rather rapidly and depart from those of the airplane. These larger phase lags at high frequencies are attributed to power saturation of the first vertical motion servo and could be corrected by using a servo having higher power output capabilities. Actually, the phase lags shown for the simulator in figure 10 were measured for a normal acceleration range of $\pm 0.4g$ at 1 cycle per second. In performing the normal task of the present study the pilot did not exceed incremental normal accelerations of $\pm 0.1g$ and therefore in normal operation the simulator phase lags at high frequencies are somewhat less than those shown by figure 10. The phase lags associated with the high-frequency pitching motions of the cockpit are considerably less than those shown by figure 10 for the normal-acceleration mode of motion.

A considerable quantity of measured frequency response and other static calibration data not shown herein were obtained during calibration

of the NAP simulator and some of the important results from these measurements are discussed.

A very small dead spot exists between stick deflection and chair response which varies directly with control-system gear ratio. The largest dead spot, ±1/16 inch of stick motion, occurs with the largest gear ratio used which was 4.5° of stick rotation for 1° of "stabilizer" rotation. (1° of stick motion is equal to 0.45 inch of stick grip travel.) The feel springs are connected directly to the stick and therefore the dead spot between stick force and stick motion is negligible. For the configuration with zero stick force, the very small static unbalanced moment on the stick due to its own weight was statically counterbalanced by means of a small bungee. The static friction in the control system is extremely small (less than 4 ounces) and is therefore considered to be negligible.

INSTRUMENTATION

Standard NASA instruments were used to measure stick position and stick force, and quantities pertaining to the cockpit itself such as rotational and vertical positions, velocities, and accelerations. The instrumentation employed to measure both absolute and integrated error between the cockpit and the target consisted of three synchrogenerators - one for target position, one for cockpit height, and one for cockpit rotation. These three signals were summed electrically and fed into a galvanometer which recorded absolute error. The summed signal was also fed into an electronic counter which integrated the error over a given period of time. All the measured quantities were synchronized by a common timer. Figure 11 shows some of the instrument installation.

METHOD AND RANGE OF TESTS

As mentioned previously, part of the program consisted of a study to determine the minimum tolerable maneuvering stability. The ranges of damped natural frequency and damping ratio of the simulated aircraft for these tests are shown in figure 12. Curves for two amounts of physical damping are shown in the figure, one for a moderate amount of damping and one for very light damping. These quantities are shown as functions of the parameter stabilizer angle per g δ_T/g. This parameter was chosen as a basic plotting quantity because it is linearly related to maneuver margin and because it does not vary with the stick gearing changes that were studied in this investigation. Throughout this investigation the steady-state normal-acceleration response in g per degree angle of attack was held at 1.0. Also the control effectiveness in terms of the

pitching acceleration produced per unit of stabilizer angle $\ddot{\theta}/\delta_T$ was held constant at 40 radians per second squared per radian of stabilizer angle δ_T. For an aircraft the corresponding quantity can be calculated by dividing the actual pitching moment produced per radian of stabilizer angle at any given flight condition by the aircraft moment of inertia measured about the Y-axis. One other important parameter defining the simulator test conditions is the ratio δ_T/α. For the most forward center-of-gravity condition tested this ratio was always 1.0 and, as the center of gravity was moved rearward, this ratio was decreased linearly with the parameter δ_T/g. Actually, it is impossible to quote a specific range of center-of-gravity positions covered in these tests unless some specific aircraft configuration is chosen. However, if a configuration similar to a present-day jet fighter airplane is assumed, the maneuver margins would range from about 15 percent mean aerodynamic chord to about -5 percent mean aerodynamic chord. It may be noted that the period and damping curves are closely representative of those for present-day fighters flying at high speeds.

Three values of control-system gearing δ_S/δ_T were tested: a fairly sensitive value of 1.13 deg/deg, a medium value of 2 deg/deg, and an insensitive value of 4.5 deg/deg. With each of these gearings, three force gradients were tested: 0, 11, and 240 pounds per inch of stick motion. The force per g for each of these springs and gearings with various amounts of stability are shown in figure 13.

The simulated flying task should not be confused with a long-range tracking task but does represent a close-formation flying or refueling type of operation. In this connection it should be pointed out that close-formation flying is intrinsically more difficult than long-range tracking because a pilot is required to supply about 90° of extra phase lead to achieve "equal" success in the former as compared with the latter. This phase lead is necessary in flying formation because the pilot is required to control altitude whereas a long-range tracking task requires attitude control.

For the present tests a repeatable trapezoidal wave form target motion was chosen. A typical time history of this motion is shown in figure 14. As can be seen in the figure the target-dwell time at the top and the bottom of the travel was adjusted to be very nearly 4 seconds. The velocity of the target was adjusted to be $2\frac{1}{3}$ feet per second with a total displacement of $4\frac{2}{3}$ feet. This particular motion was chosen after considerable trial and error. It was not considered desirable to present to the pilot such a simple task that he would be able to perform the task with even very poor airplane characteristics. On the other hand, an

extremely difficult task was considered equally undesirable because the pilot would not be capable of performing such a task even with good characteristics. It should be noted that this task is a very critical one requiring extreme precision of the pilot and control system.

For each stability setting the pilot was allowed to practice for a short period (usually a few minutes were sufficient) so that he could become somewhat familiar with the characteristics involved. At the end of this practice period, a test run would be recorded. Each data run lasted for an interval of 1 minute during which time communication ceased. This procedure was followed so that the pilot could concentrate solely on the task. It should be noted that no tasks were involved other than keeping the sighting image alined with the target. For each spring and stick to stabilizer gear ratio tested, the stability was reduced in small increments until the point was reached that the pilot could no longer control the simulator. The number of data points obtained varied somewhat with configuration because the pilot could tolerate less stability with configurations having good control characteristics. With the better configurations, approximately 12 data points were obtained.

The pilot's performance was judged primarily on the basis of the integrated absolute-error measurement. This integrated error was used in the calculation of a quantity called "performance index." All the basic test data are therefore plotted in the form of performance index as a function of the stability parameter stabilizer angle per g. The performance index is defined as follows:

$$\text{Performance index} = \frac{\text{Error}_{\text{cockpit motionless}} - \text{Error}_{\text{actual}}}{\text{Error}_{\text{cockpit motionless}}}$$

If a pilot was able to keep the sighting image perfectly alined with the target at all times during a 1-minute test run, his performance index would be 1. If, however, the pilot did not try to follow the target at all but instead held the sighting image in the center of the target travel (cockpit motionless), his performance index would be 0. If the target and the sighting image were out of phase (that is, when the target went up the sighting image went down), the performance index would be negative. It is inconceivable for any human being to perform with the precision necessary to produce a performance index of 1. This would require zero lag in the human's neuromuscular reaction and also perfect leading and integrating capabilities. A more logical idealistic performance was calculated theoretically and is shown in the form of a time history of sighting image or cockpit position in figure 14. When this time history was calculated, a total constant time lag of 0.5 second was assumed for

the combined pilot, control system, and airplane dynamics. Such an idealistic performance would produce a performance index of 0.80. Actual performance indices would therefore generally be expected to be somewhat less than 0.80.

In connection with the choice of target motion, a very simple repeating motion rather than a complex random motion was purposely chosen in the belief that such a simple motion would allow the most clear-cut isolation of the effects of the aircraft stability and control characteristics under study. Even though the pilots could quickly memorize the task, the possible advantage gained thereby had little effect on the overall results especially for the cases in which the stability of the simulated aircraft was near the neutral stability region.

Two NASA test pilots served as simulator pilots for all the tests presented in this paper.

RESULTS AND DISCUSSION

Representative sample time histories of a portion of a test run with each pilot are shown in figure 15 to illustrate the slow and deliberate technique used by the pilots. For both of these runs the force gradient was 11 pounds per inch of stick motion, the gear ratio was 2.0 degree stick rotation per degree tail deflection and the maximum amount of aircraft stability was used together with the moderate amount of damping. This slow technique usually prevented large overshoots and ensuing oscillations when the target stopped. Prevention of such overshoots is evidently considered by pilots to constitute good piloting technique because, generally speaking, most experienced pilots strived for this goal.

Effect of Aircraft Damping

The first part of the test program was devoted to a study of the effect of two amounts of aircraft damping on pilots' performances. The two amounts of damping were discussed previously and are shown in figure 12. The results of the damping tests are shown for one pilot in a plot of performance index against stabilizer angle per g in figure 16. The results with the other pilot were so similar they are not presented herein. As can be seen in figure 16, reducing the damping from the moderate to light value caused a reduction in performance index over the entire stability range covered and the pilot could tolerate less maneuvering stability with the larger amount of damping. The difference between the performance curves is not as large as might have been expected

and, indeed, the pilots commented that the decrease in damping made the configuration slightly less desirable but they did not feel that the effects were of a very serious nature. It should be pointed out that such comments could depend greatly on the fact that the pilot was concerned with only one task. It is possible that, if the pilot was required to divide his attention among the many tasks involved in actual flight, the reduced damping effect may be far more serious.

Effect of Force and Position Gradients

During the damping tests most of the pilots' comments were directed at the extremely light stick forces and the increase in the sensitivity of the control stick as the stability was decreased. These comments suggested the possibility of improving performance by increasing the stick force or stick motion or a combination of the two; therefore, tests were made to study the effects of large changes in force gradient and position gradient. For these tests the "moderate" damping condition of figure 12 was used. Three force gradients were tested - 0, 11, and 240 pounds per inch of stick motion. These force gradients were tested in conjunction with each of three stick position gradients or control-system gear ratios, 1.13°, 2.0°, and 4.5° of stick motion per degree of stabilizer angle. (See fig. 13 for associated force per g values.) It should be mentioned that preliminary tests were made with two other force gradients, 90 and 820 pounds per inch. The performances with these gradients, however, were inferior to the performances with the 240 pounds per inch gradient. Therefore, the gradient of 240 pounds per inch was chosen to represent the high force gradient in this investigation.

The basic data from the tests of various force and position gradients throughout the stability range are shown for the two pilots in figure 17. These data are presented in the form of plots of performance index against stabilizer angle per g. Also shown at the top of the figures are scales for aircraft period and damping ratio to show how these associated parameters varied. The maneuver point $\delta_T/g = 0$ is shown by a vertical line. The points to be noticed in this figure are the comparison between the two pilots, the performance levels between configurations, and the least amount of stability that could be tolerated with each configuration. The last point on each curve was the least stability for which successful runs could be made. The effect of position gradient or control-system gearing can be seen by comparing the individual figures for each pilot. The effect of force gradient is shown by the three curves in each figure. Such comparisons show that increasing the gearing from 1.13 to 2.0 resulted in some improvement for the cases when forces were present. Further gearing increases for these cases showed no improvement. With zero forces, increasing the gear ratio resulted in a slight improvement in performance level for the maximum stability condition with pilot A.

Increased gearing improved pilot B's performance throughout the stability range. Also with zero forces and gear ratios of 2 and 4.5 the pilots could tolerate less stability than they could with the more sensitive gearing of 1.13. During the tests with zero forces the pilots commented that control was somewhat easier with the higher gear ratios; however, they did not feel at the time that the performance levels would be affected. Increasing the force gradient to 11 pounds per inch produced noticeable improvements in both the measured performance and pilot comments. It should be pointed out here that the gradient of 11 pounds per inch gives values of force per g which agree closely with the gradients specified in present-day flying-qualities requirements for gross maneuvers with fighter airplanes. (See fig. 13.) However, even with this force gradient the pilots felt that the forces were far too light when the aircraft was only weakly stable. As shown in figure 13, control was possible with this force gradient with extremely weak stability and in some cases with neutral stability; however, the performance in this region was only a little better than if the pilot made no attempt to follow the target. With a spring force gradient of 240 pounds per inch on the stick the performance level was improved in most cases throughout the entire stability range but the most noticeable improvement occurred in the region of neutral stability. In fact, with this high gradient the pilots could consistently control the simulator with a small degree of instability. These effects are probably more easily recognized in figure 18, where the performance index is plotted as a function of control-system gear ratio for the three force gradients tested. The beneficial effects of the high force gradient are more obvious in this figure, especially in the region of neutral stability, due to the fact that in the last plot on these figures only the curve for the force gradient of 240 pounds per inch is present. What the data do not show is the improvement in ease of controllability at neutral stability from the pilot's viewpoint. Even though these extremely high forces provided a large improvement in these tests, it should be remembered that the task involved is one of extreme precision requiring very small stick motions; therefore, the reader should not infer that such gradients are hereby proposed for gross maneuvering.

With regard to pilots' comments on the use of the stick force gradient of 240 pounds per inch, some amplification is in order. At large real stability (large values of δ_T/g), the pilots considered the forces far too heavy. Even though they could produce very good performances, they often employed both arms for control and even then became unduly fatigued in periods as short as 5 minutes. At zero stability, on the other hand, the forces were considered to be just about optimum. The large improvement in performance that was obtained at the maneuver point by use of the very heavy spring is attributed to the increase in precision which could be attained by the pilots in positioning the stick. With very light springs or no springs at all, loss of control and the ensuing "crash" always appeared to result from inadvertent overcontrolling.

As the stability was reduced, the pilots were forced to concentrate more and more on stabilizing the simulator rather than on following the target. This effect was most pronounced for the cases of near-neutral stability with light force gradients or with no force at all. Figure 19 shows a typical time history made with these conditions. The figure illustrates that for these cases the target was all but ignored and practically all the pilot's attention was directed toward preventing a crash. The resulting performance indices measured for such cases were very nearly zero. For the same real stability conditions but with a force gradient of 240 pounds per inch, the simulator was much easier to stabilize; thus, the pilot could apply more attention to the task and consequently produce higher performance indices. Figure 20 shows a typical time history made with these conditions.

On the basis of the foregoing tests, the pilots concluded that, in general, the maneuver point constitutes a reasonable rearward limit beyond which the center of gravity should never be allowed to move for vehicles controlled directly by a human pilot without the assistance of any type of stability augmentation equipment. When the control feel forces were very low or absent, sustained flight at the maneuver point was indicated to be impossible. When the control feel forces were high, sustained flight, even with negative stick-fixed maneuvering stability, was indicated to be possible; however, such flight was not considered to be practical because any diversion of the pilot's attention from the one task of maintaining longitudinal control usually resulted in loss of control. The use of control-feel systems more sophisticated than the simple spring type employed herein may, of course, modify the foregoing conclusion to some degree.

Pitching-Motion Test

After the force and position gradient tests were concluded, some additional tests were made in an attempt to determine whether the pitching motion played an important part in the pilot's ability to perform the task. Therefore, each pilot made several runs, some with the pitch system operating and some with the pitch system turned off. For these runs the force gradient was 11 pounds per inch and the control-system gear ratio was 2.0. The results from these tests are shown in figure 21, which includes the data with both pilots. The method of obtaining these data consisted of making one run at a given stability with the pitch servos on, and then the run was repeated at the same stability with the pitch servos turned off. This procedure was followed for each successively smaller degree of stability until controlled flight was no longer possible. As shown in figure 21(a), pilot A performed about as well with the pitch system off as he did with the pitch system on. Pilot B, however, as shown in figure 21(b), showed a very slight improvement with the pitch system on. Both pilots commented that the

overall motion of the simulator was a little smoother when the pitch system was operating. This effect was most noticeable during the target-dwell time when the pilot was attempting to stop the sighting image on the target. During these periods the simulator performed very small-amplitude oscillations and it is believed that the more numerous oscillations that occurred in the absence of pitching motion are the direct cause of the slight difference measured in performance index. In general, then, these results indicated that the pitching motion supplied a smoothing effect on the overall simulator motion and therefore made the simulation more realistic. Performancewise, however, the pitching-motion effect was very small if not negligible.

Effect of Piloting Technique

It was noticed during these pitch tests that pilot A had used an entirely different piloting technique. Instead of the slow and deliberate technique that he employed in the previous tests, he was much more aggressive. This so-called "desperation" technique involved much higher vertical velocities of the chair and, consequently, when the target stopped, the pilot would overshoot and set up small-amplitude oscillations even with the pitch system operating. An example time history of a portion of such a test run is shown in figure 22. These oscillations would normally tend to lower the performance level but the high vertical velocities used by the pilot kept the sighting image more closely alined with the target when the target was moving. As shown in figure 21(a) this desperation technique resulted in considerably higher performance indices than were measured in any of the previous runs; in fact, pilot A exceeded the predicted performance level of the "theoretical" pilot discussed earlier (Performance index = 0.80) in at least 4 runs. Pilot A commented, however, that he would never employ such a technique in actual flight because of the increased possibility of losing control.

The foregoing results suggested the possibility that higher force gradients might not improve performance if the pilot used this desperation technique because the higher forces might tend to prevent fast stick motions. Therefore, additional runs were made with pilot A with a force gradient of 240 pounds per inch. The pilot was instructed to use the same desperation technique for these runs and the results are shown in figure 23. This figure shows that the high force gradient resulted in about the same amount of improvement as was measured with the normal piloting technique discussed earlier. These tests, therefore, proved that, regardless of technique used, very high force gradients were definitely beneficial in the absence of stability.

CONCLUSIONS

Tests have been made on the NASA normal acceleration and pitch (NAP) simulator utilizing a close-formation flying task for the purpose of studying the effects on controllability of various amounts of aircraft stability and various amounts of stick force and position gradients. From these tests the following conclusions were drawn:

1. The maneuver neutral point appeared to be a reasonable rearward limit for the airplane center of gravity for airplanes under direct control of human pilots.

2. Force gradient appeared to be the most important contributor to precise control, especially when the airplane center of gravity was near the maneuver point. The best performances in the simulated formation-flying task were obtained with force gradients many times larger than those specified for gross maneuvering for fighter-type airplanes in present-day flying-qualities requirements. Such force gradients would, however, be excessive in maneuvers requiring steady accelerations unless the center of gravity is at or very near to the maneuver point.

3. Increasing the stick position gradient from 1.13 to 2.0 improved performance throughout the stability range. Increasing the gradient to 4.5 improved performance for the cases with zero stick forces but for the cases with some amount of force gradient no improvement resulted.

4. Reducing the aircraft damping resulted in somewhat lower performance; however, this effect was not considered to be particularly serious.

5. Leaving out the pitching motion in this simulation resulted in practically no reduction in performance; however, the presence of the pitching motion had a smoothing effect on the overall cockpit motion and made the simulation feel more realistic.

6. Performance was improved when the pilot changed his method of flying from the normal slow and deliberate technique to a more aggressive or "desperation" technique. The performance with this desperation technique was also improved through the use of higher force gradients. This improvement was again most noticeable when the aircraft center of gravity was near the maneuver point.

Langley Research Center,
National Aeronautics and Space Administration,
Langley Field, Va., April 15, 1959.

REFERENCES

1. Brown, B. Porter: Ground Simulator Studies of the Effects of Valve Friction, Stick Friction, Flexibility, and Backlash on Power Control System Quality. NACA Rep. 1348, 1958. (Supersedes NACA TN 3998.)

2. Anon.: Electric-Hydraulic Gun Drives for 5"/38 Caliber Dual Purpose Mount. Ord. Pamphlet 1103, Bur. Ord., Jan. 1945.

3. Stokes, Fred H., and Mathews, Charles W.: Theoretical Investigation of Longitudinal Response Characteristics of a Swept-Wing Fighter Airplane Having a Normal-Acceleration Control System and a Comparison with Other Types of Systems. NACA TN 3191, 1954.

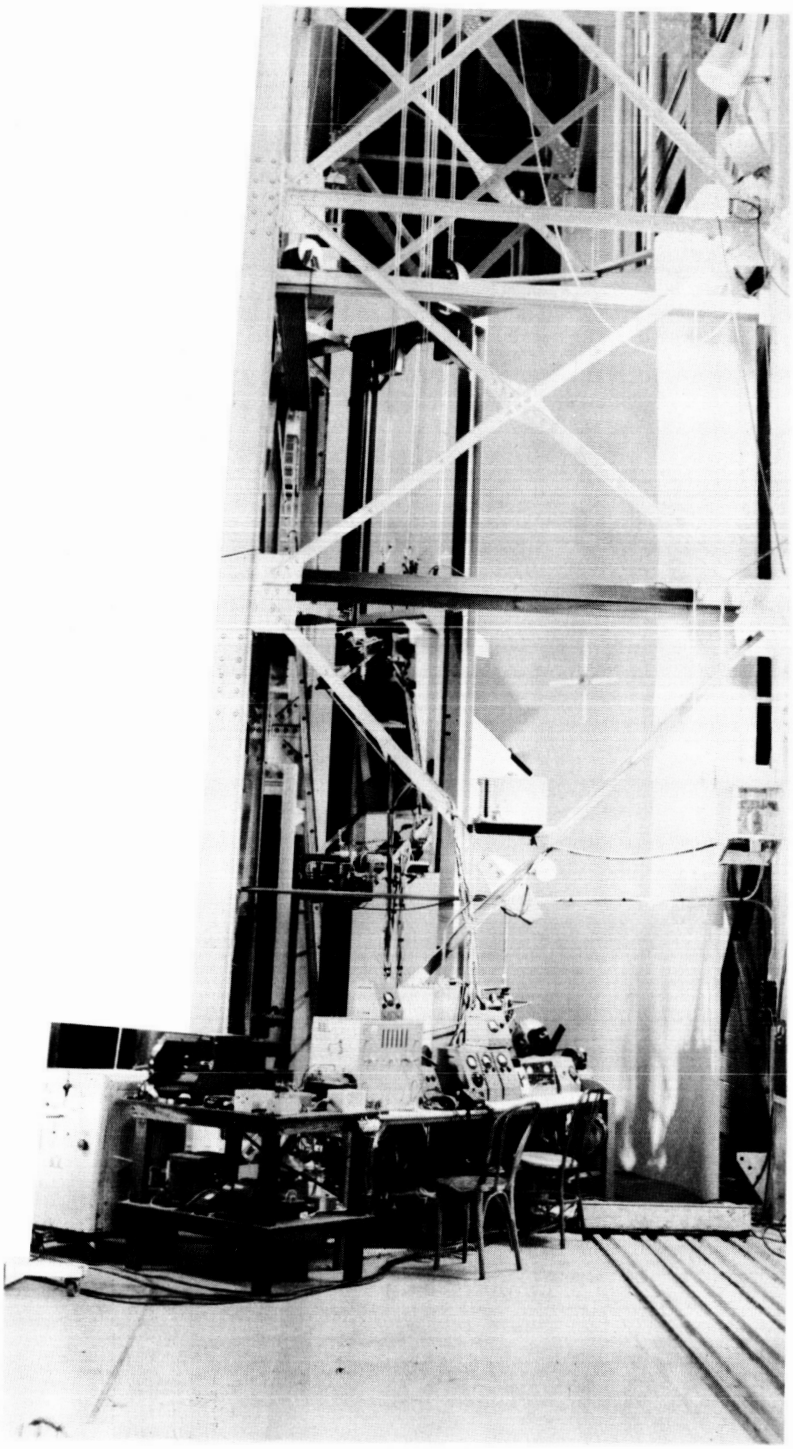

Figure 1.- Overall view of normal acceleration-and-pitch (NAP) simulator. L-58-2062

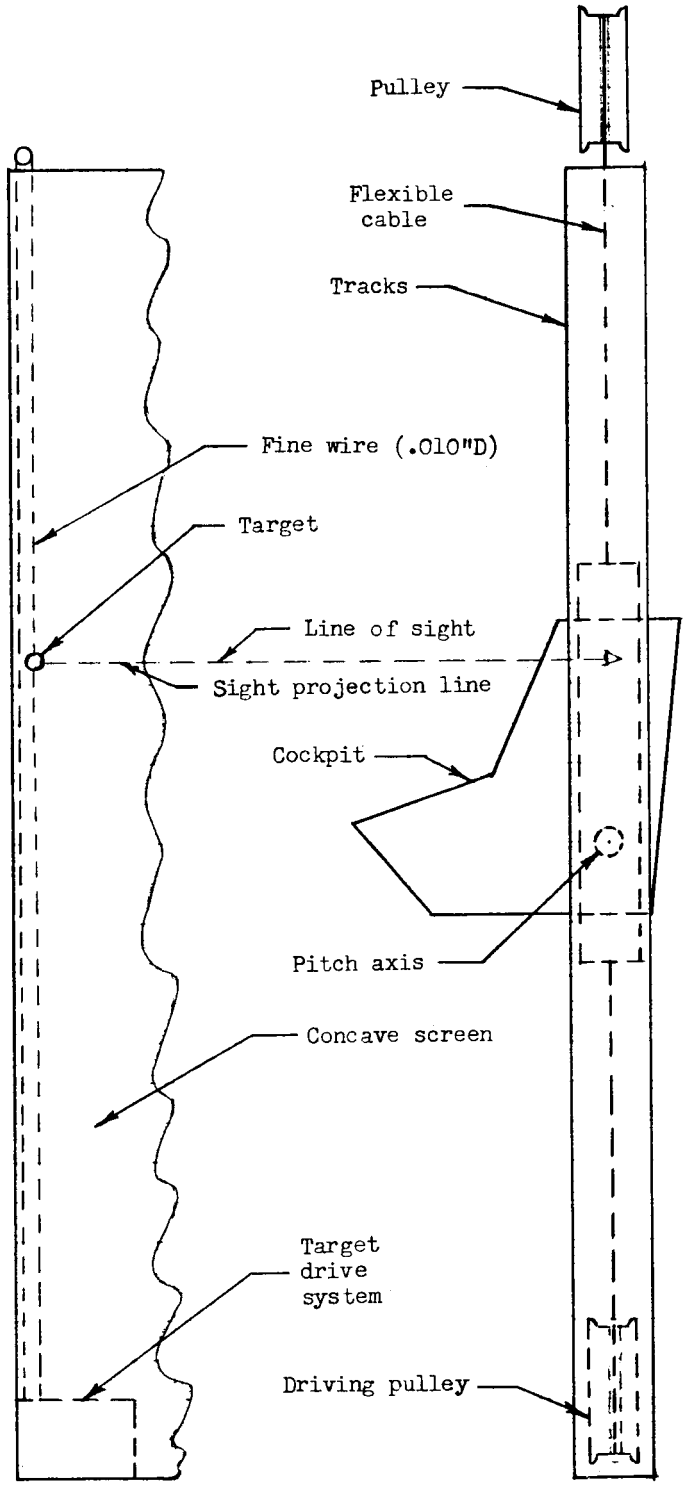

Figure 2.- Schematic drawing of the NAP simulator.

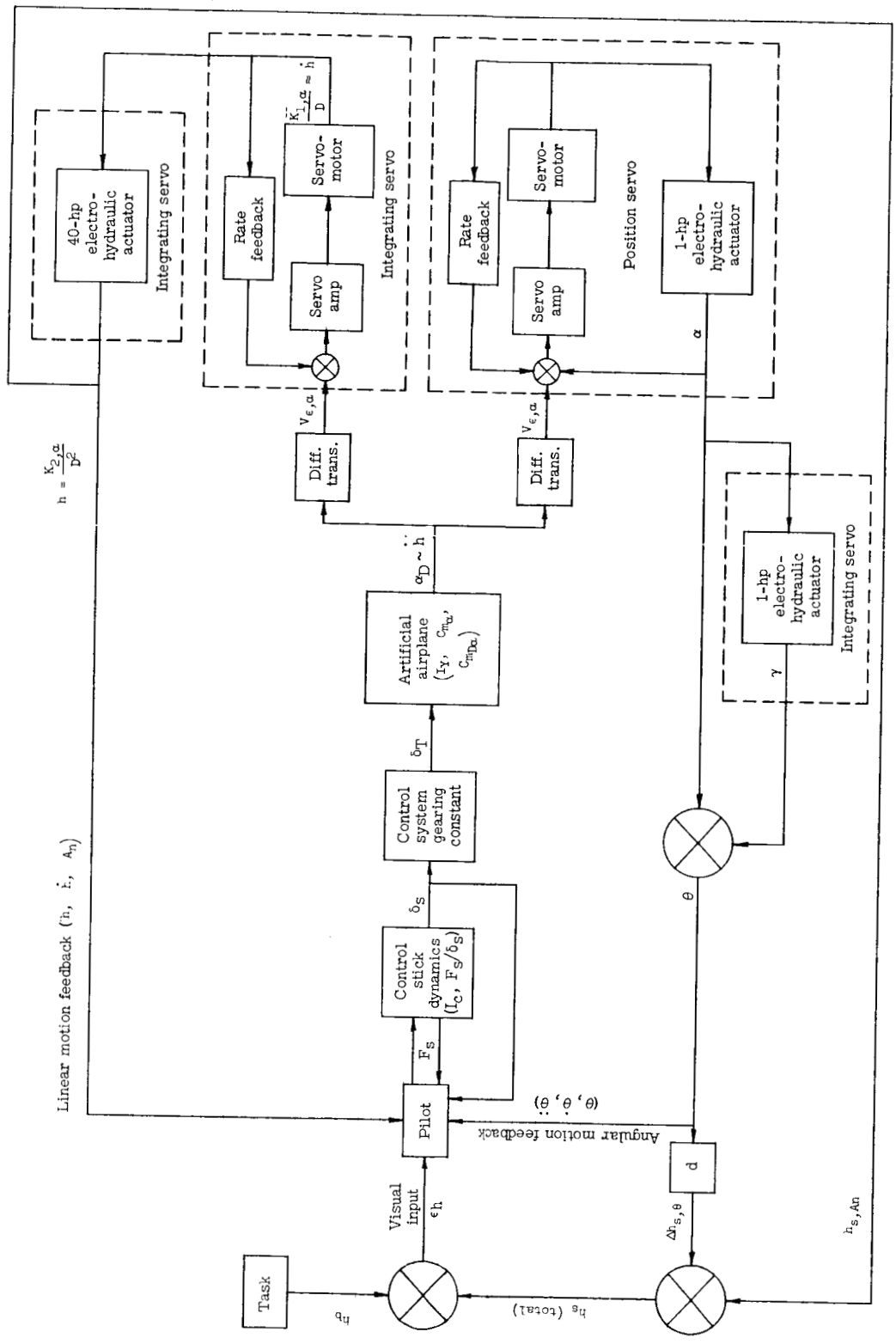

Figure 3.- Component block diagram of NAP simulator.

L-58-2069.1

Figure 4.- View of pilot seated in cockpit of simulator.

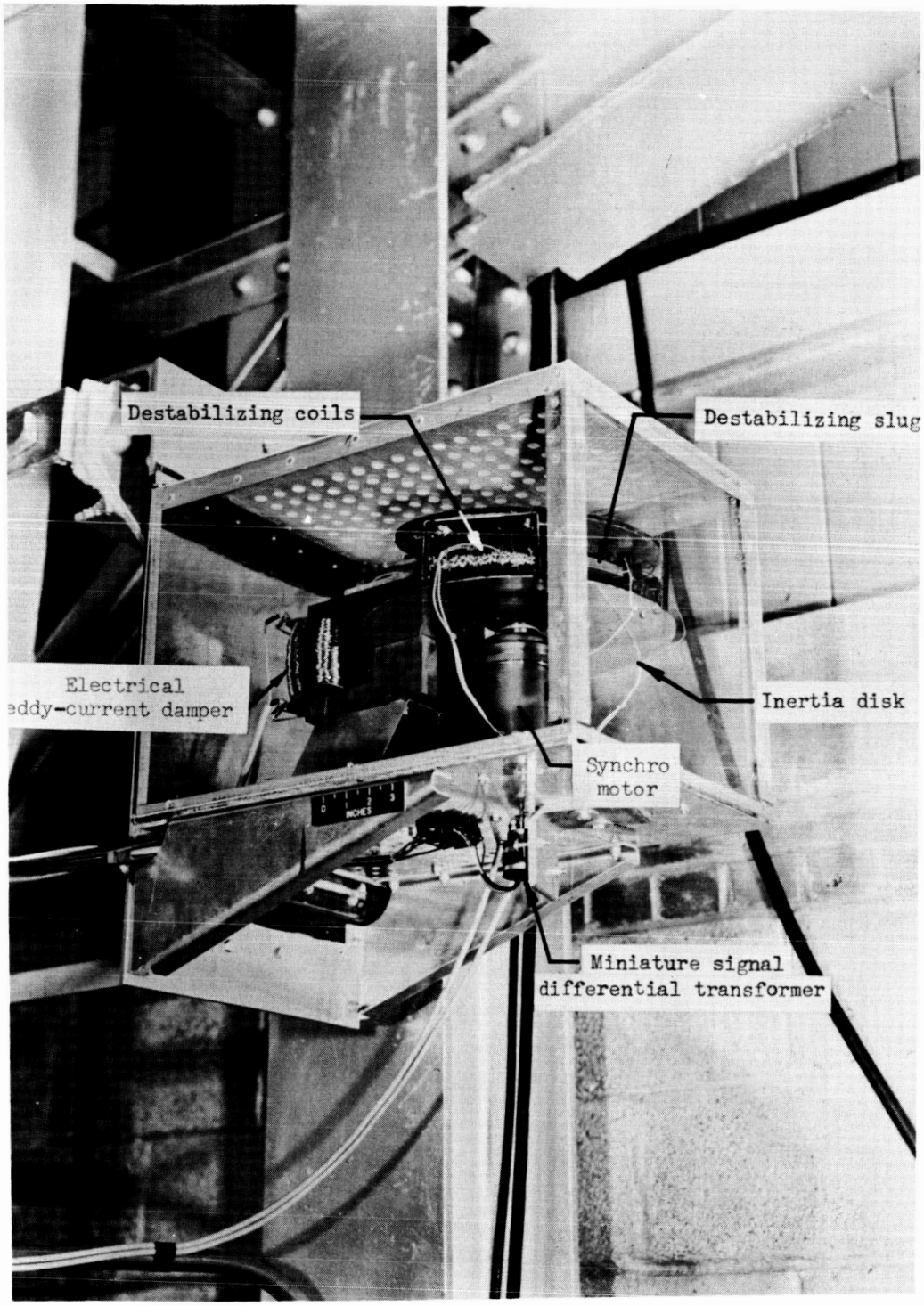

Figure 5.- "α-simulator" of NAP simulator. L-58-2063.1

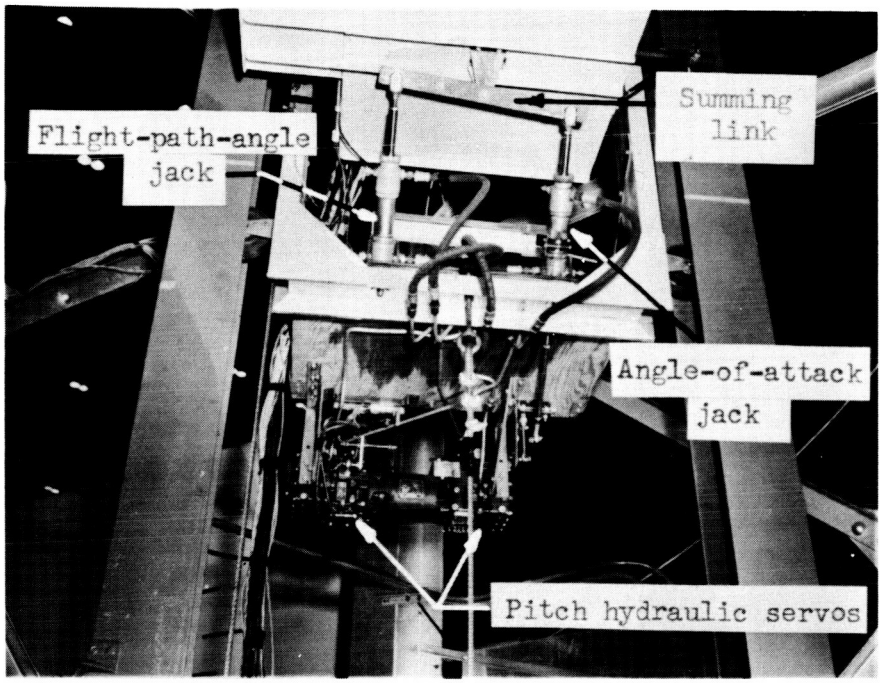

L-58-2070.1

Figure 6.- Pitch servosystem of NAP simulator.

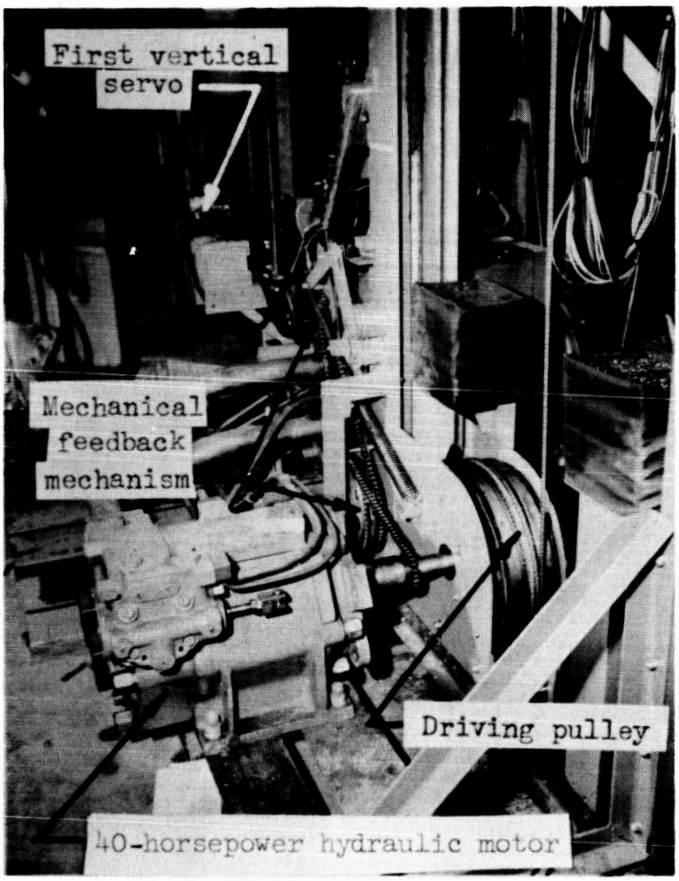

L-58-2067.1

Figure 7.- Vertical motion driving mechanism of NAP simulator.

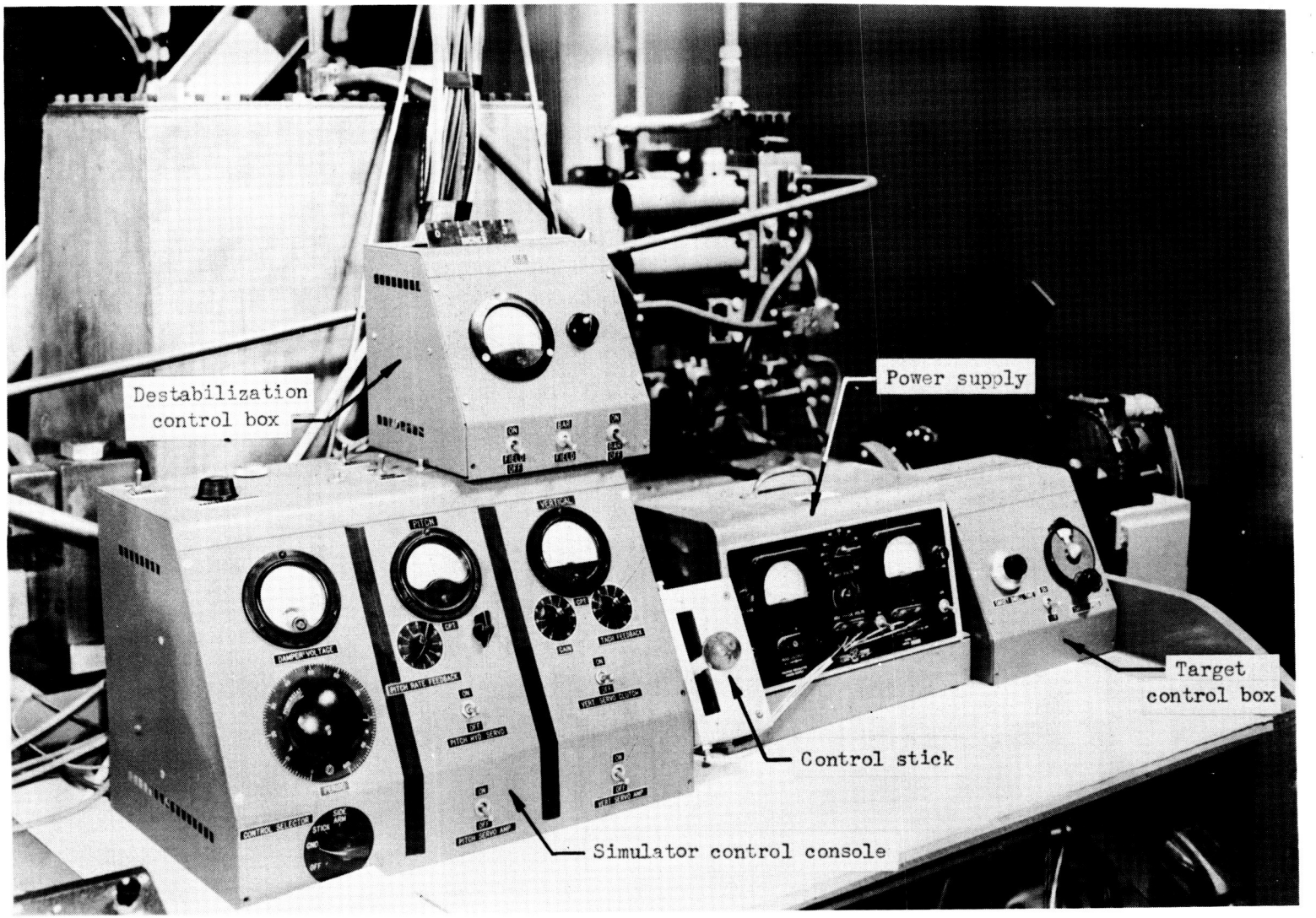

Figure 8.- Ground operator control station of NAP simulator. L-58-2065.1

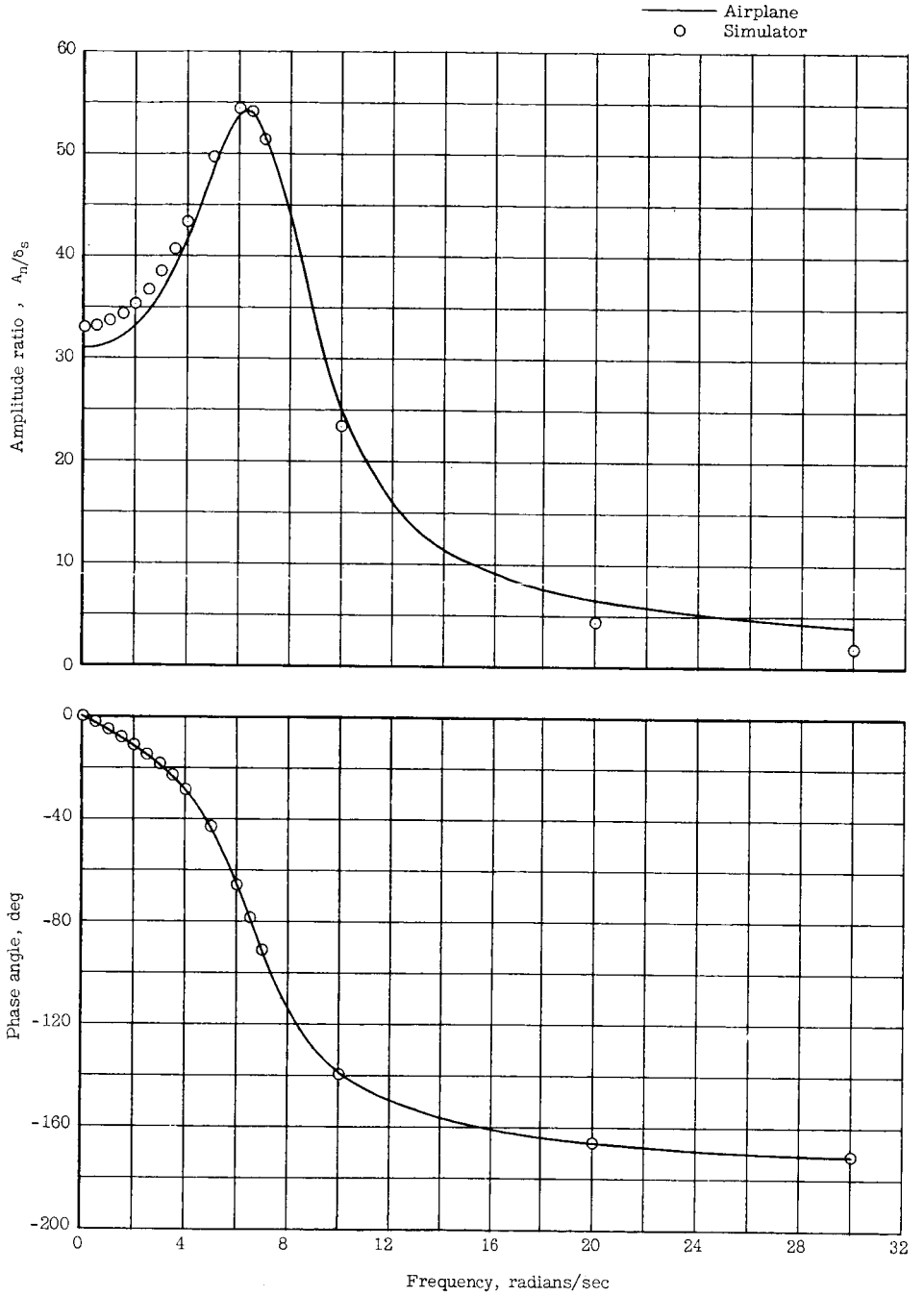

(a) Normal acceleration due to stick motion.

Figure 9.- Comparison of calculated idealized frequency responses of an airplane and the NAP simulator.

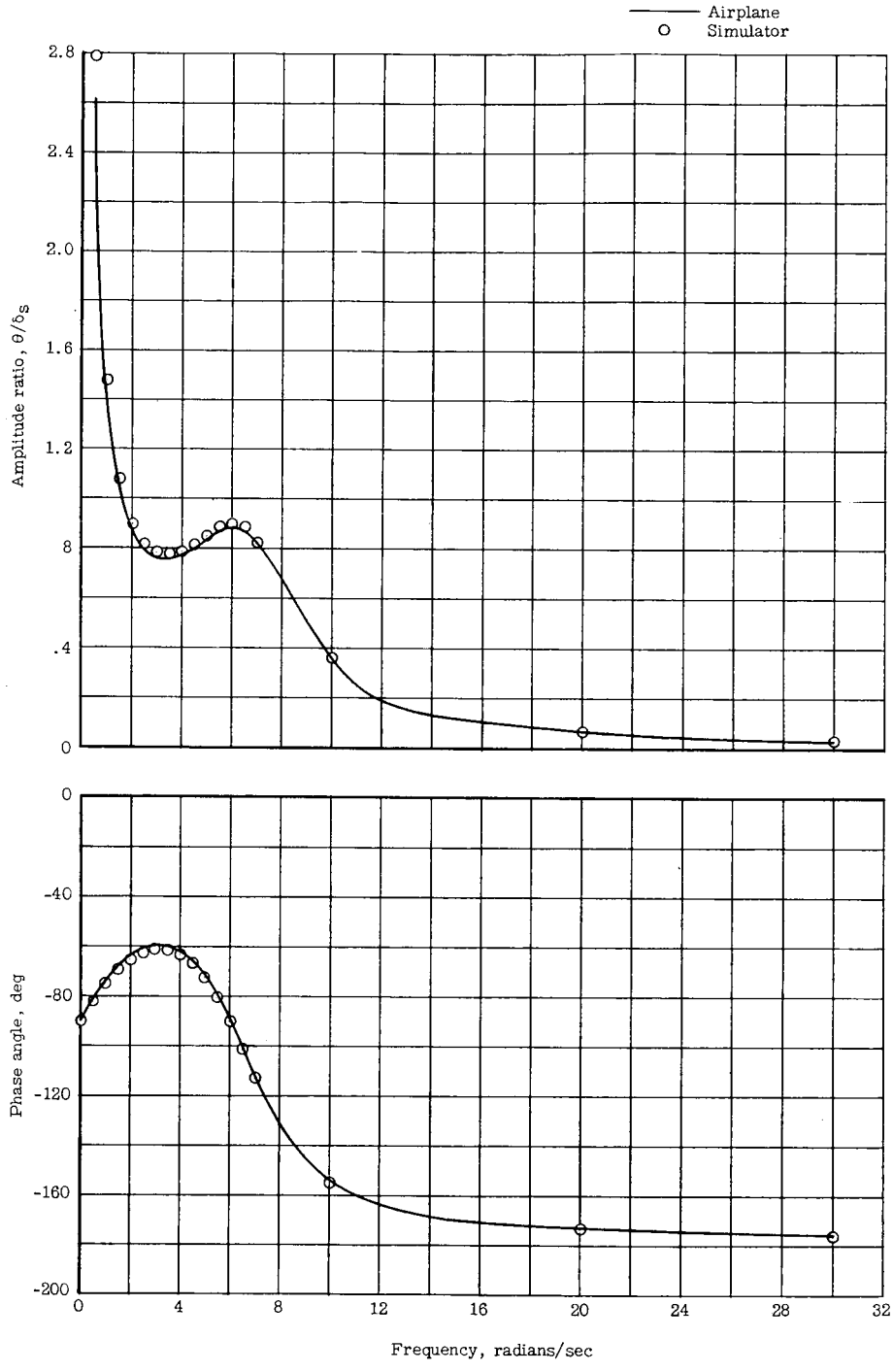

(b) Pitch angle due to stick motion.

Figure 9.- Concluded.

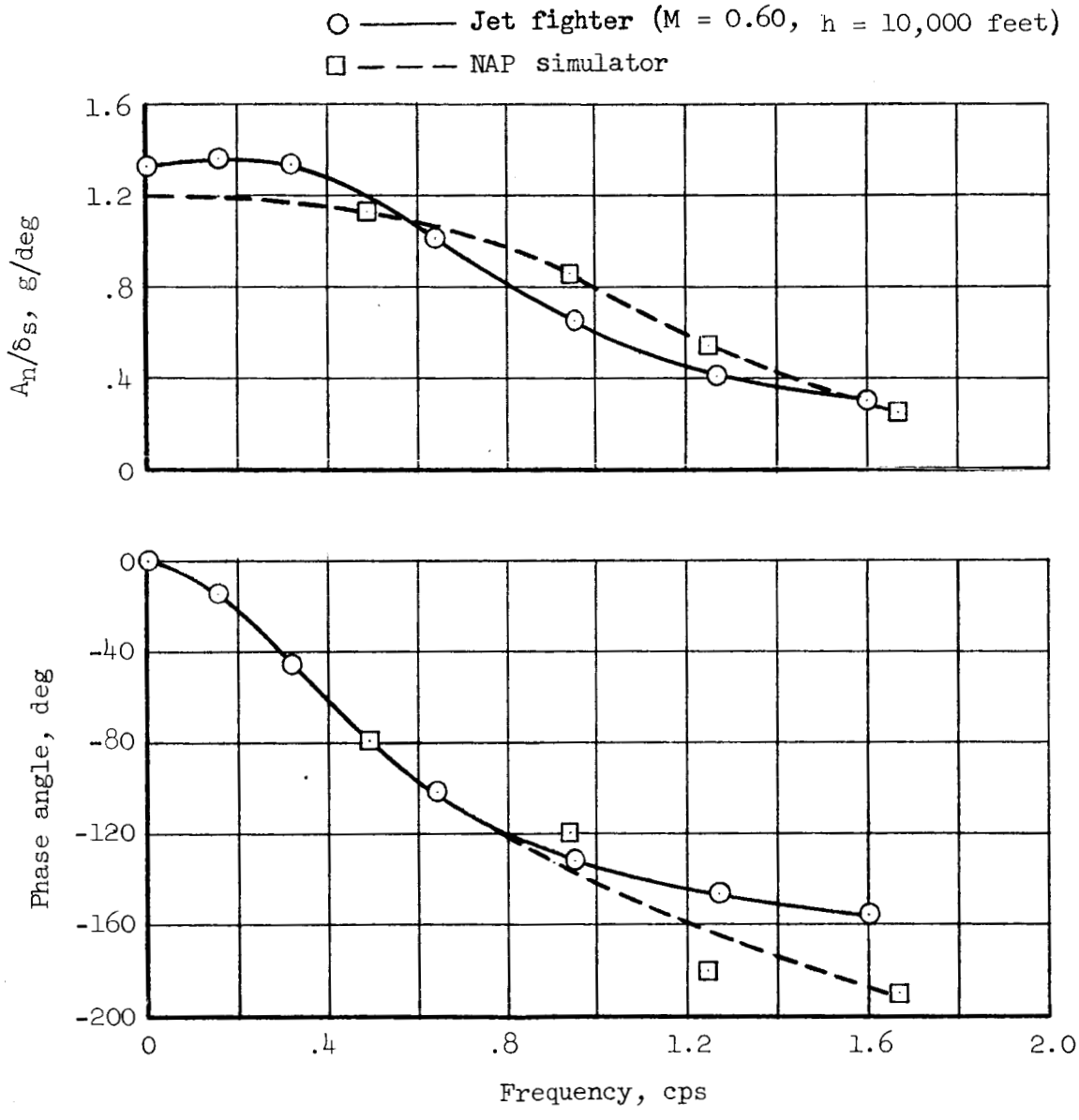

Figure 10.- Comparison of actual frequency responses of a jet fighter airplane and the NAP simulator.

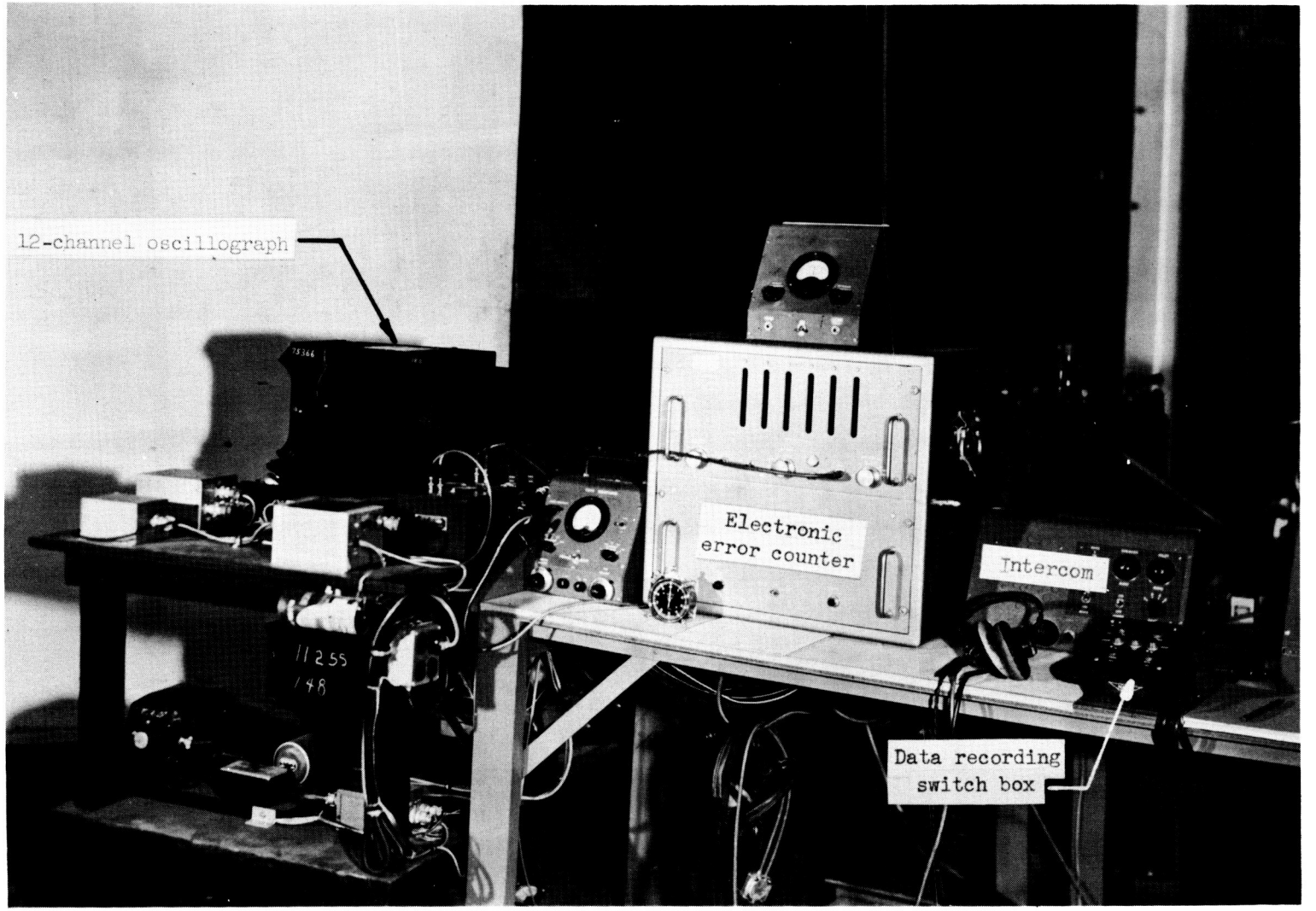

Figure 11.- Instrument installation of NAP simulator. L-58-2064.1

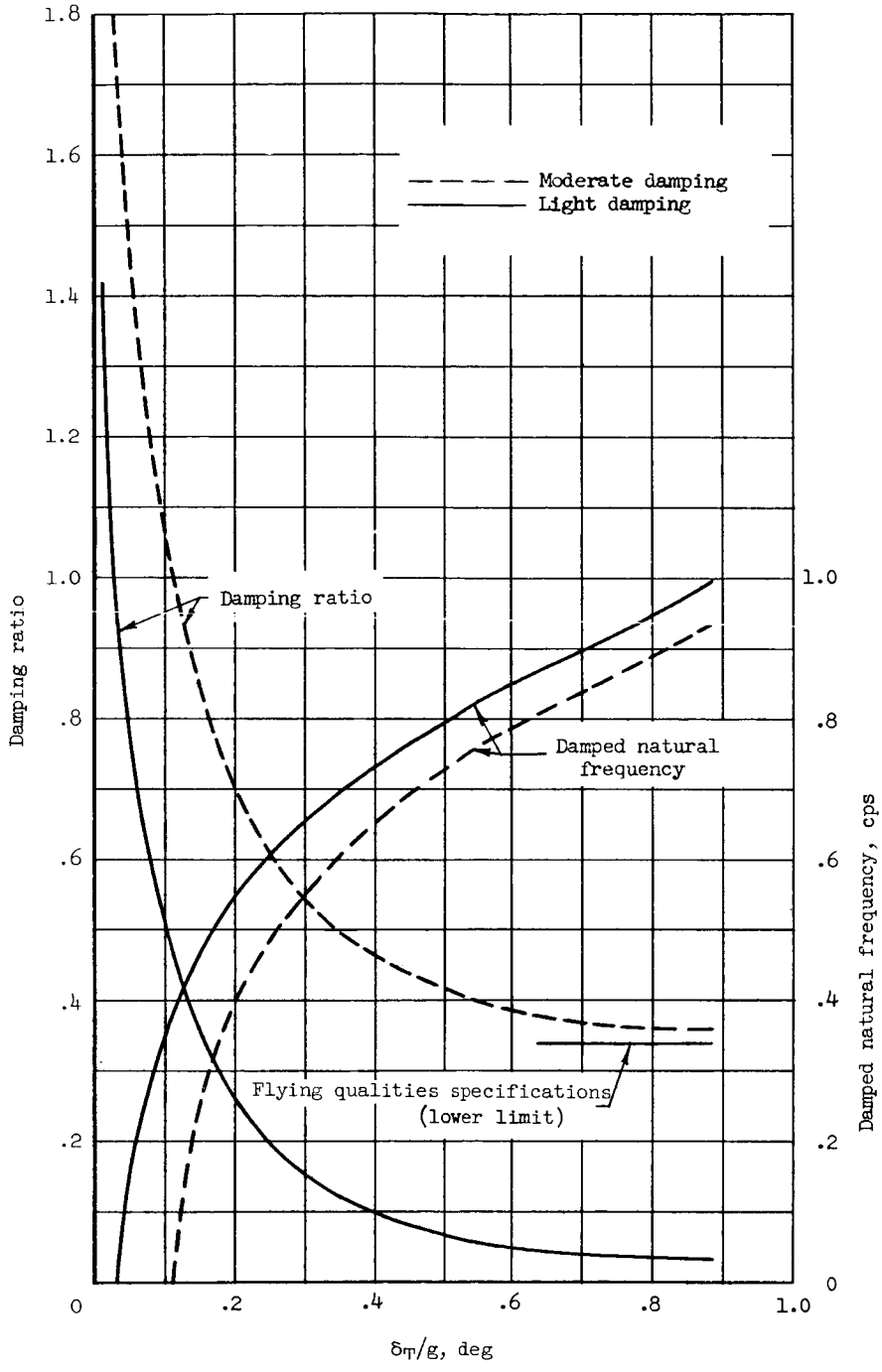

Figure 12.- Damped natural frequency and damping characteristics of NAP simulator as functions of the parameter stabilizer angle per g. Two values of physical damping are shown.

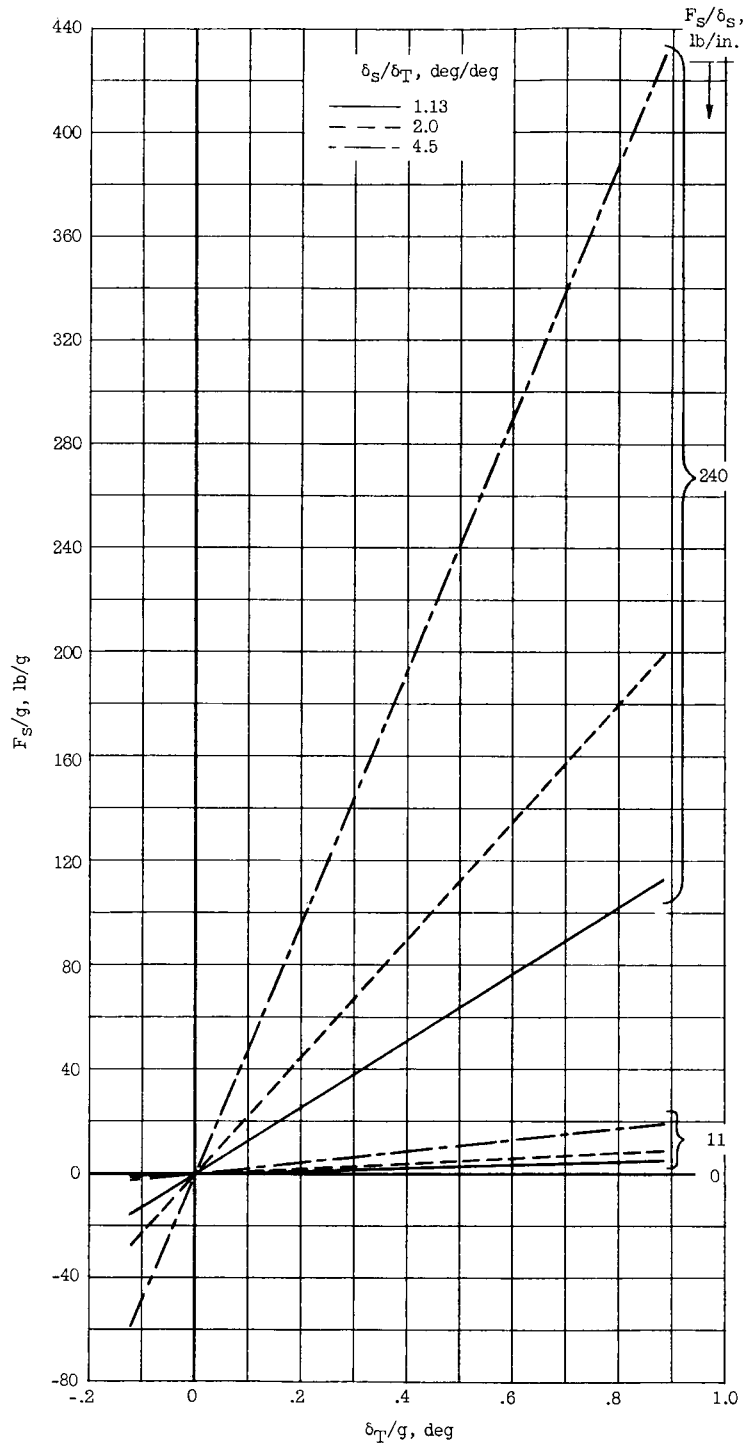

Figure 13.- Variation of stick force per g with the parameter stabilizer angle per g for various feel springs and control-system gearings.

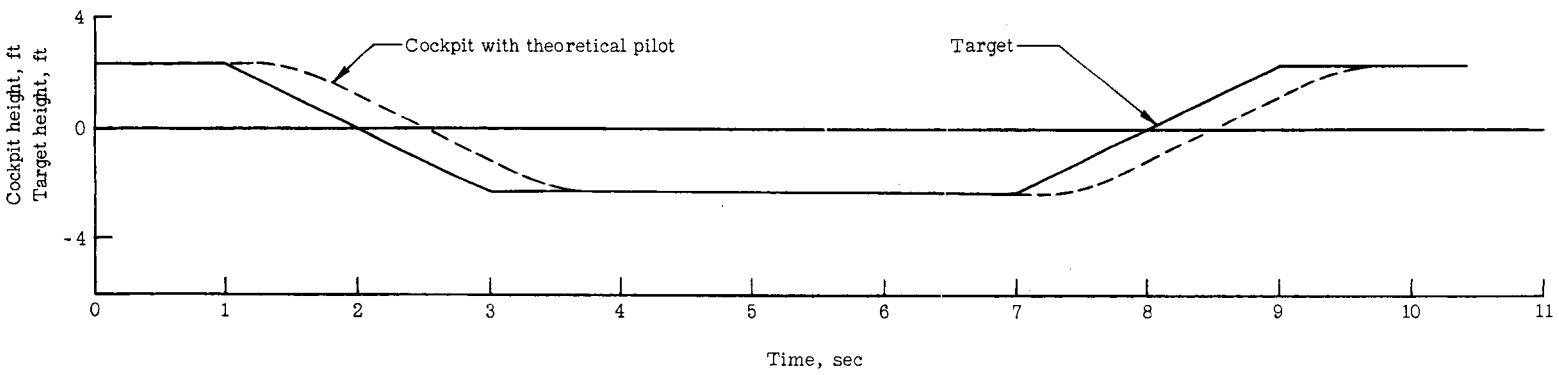

Figure 14.- Time history showing calculated performance of theoretical pilot.

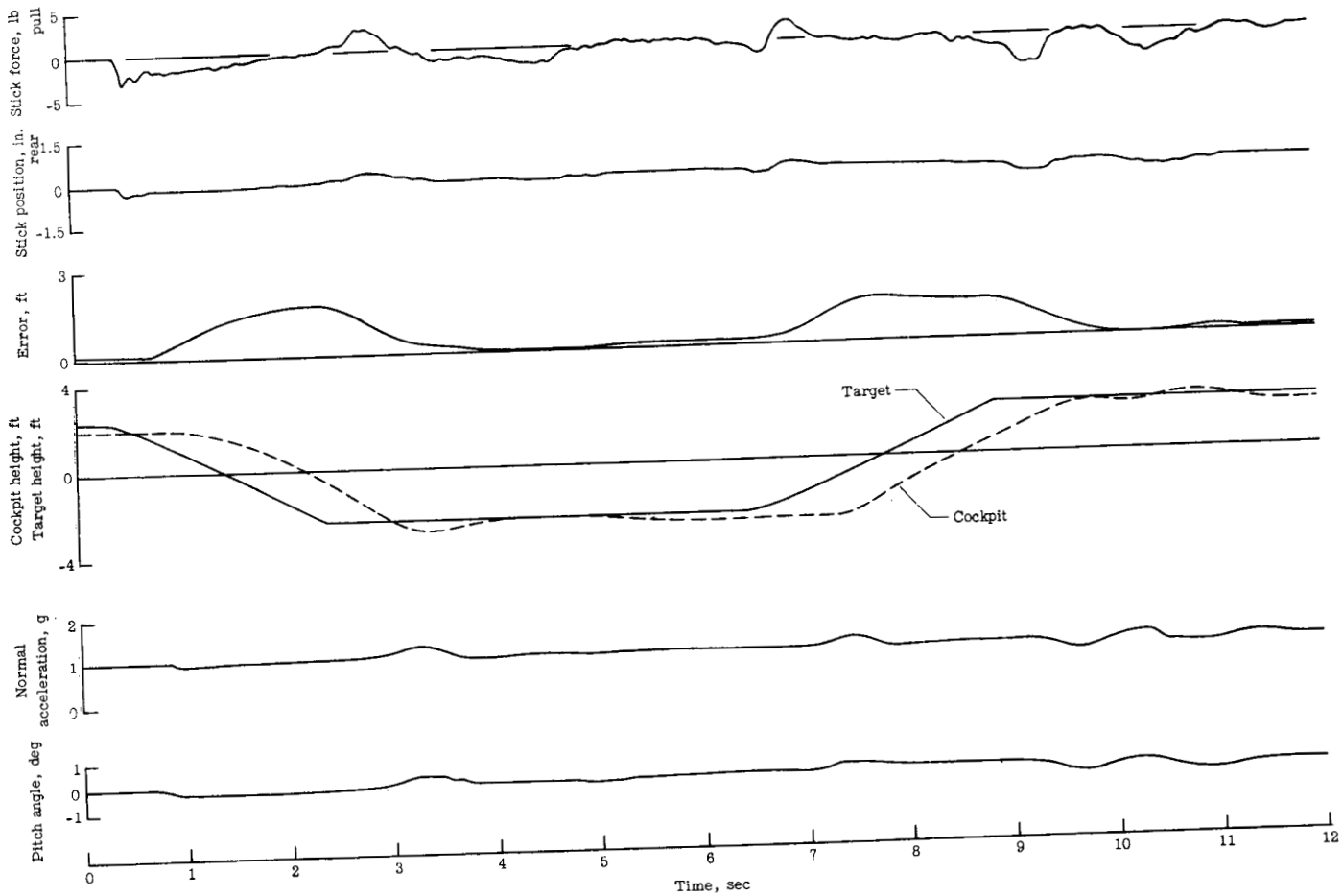

(a) Pilot A.

Figure 15.- Typical time histories showing slow technique normally used by pilots. F_s/δ_s = 11 lb/in.; δ_s/δ_T = 2.0 deg/deg; δ_T/g = 0.89; damping ratio = 0.36.

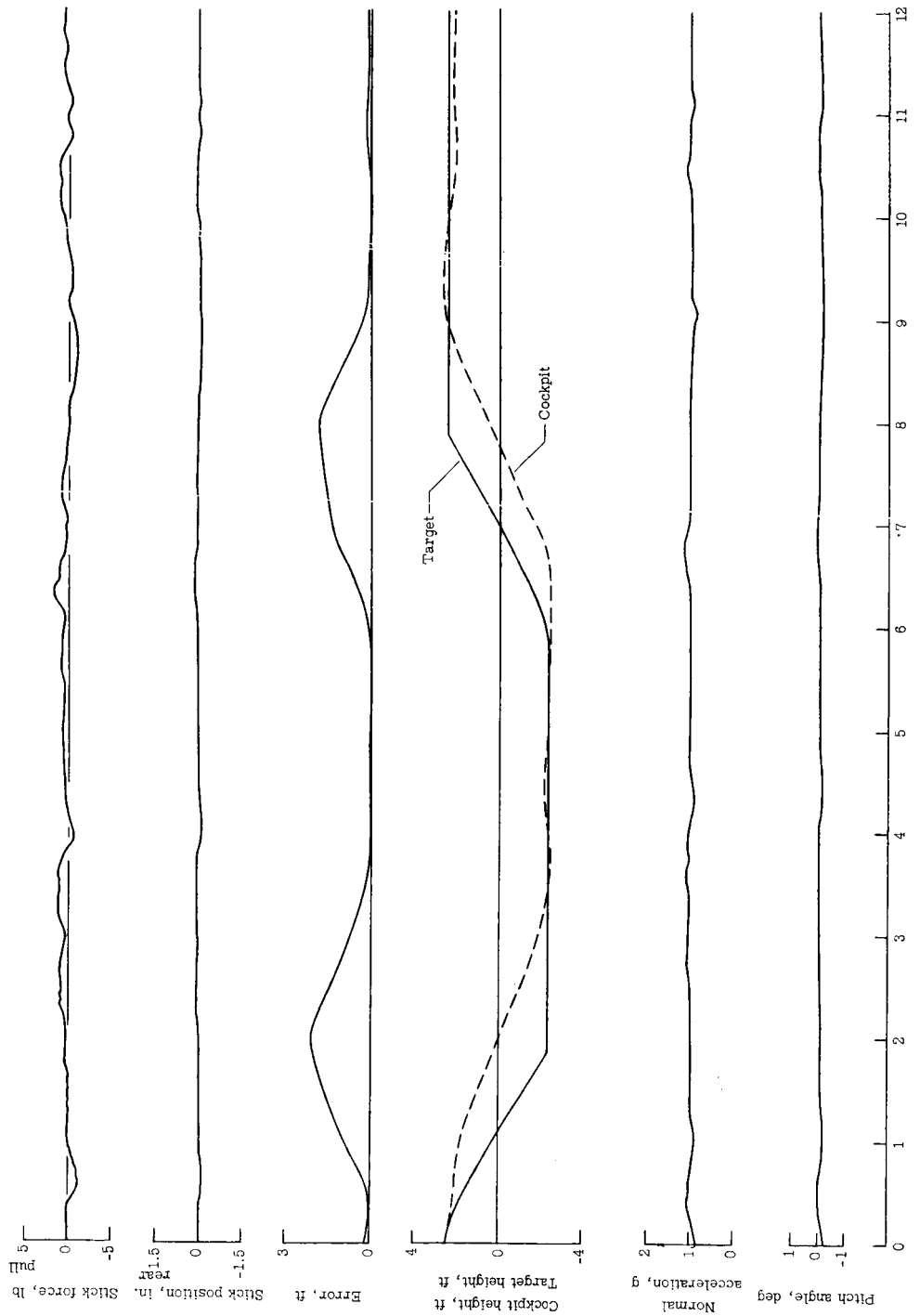

(b) Pilot B.

Figure 15.- Concluded.

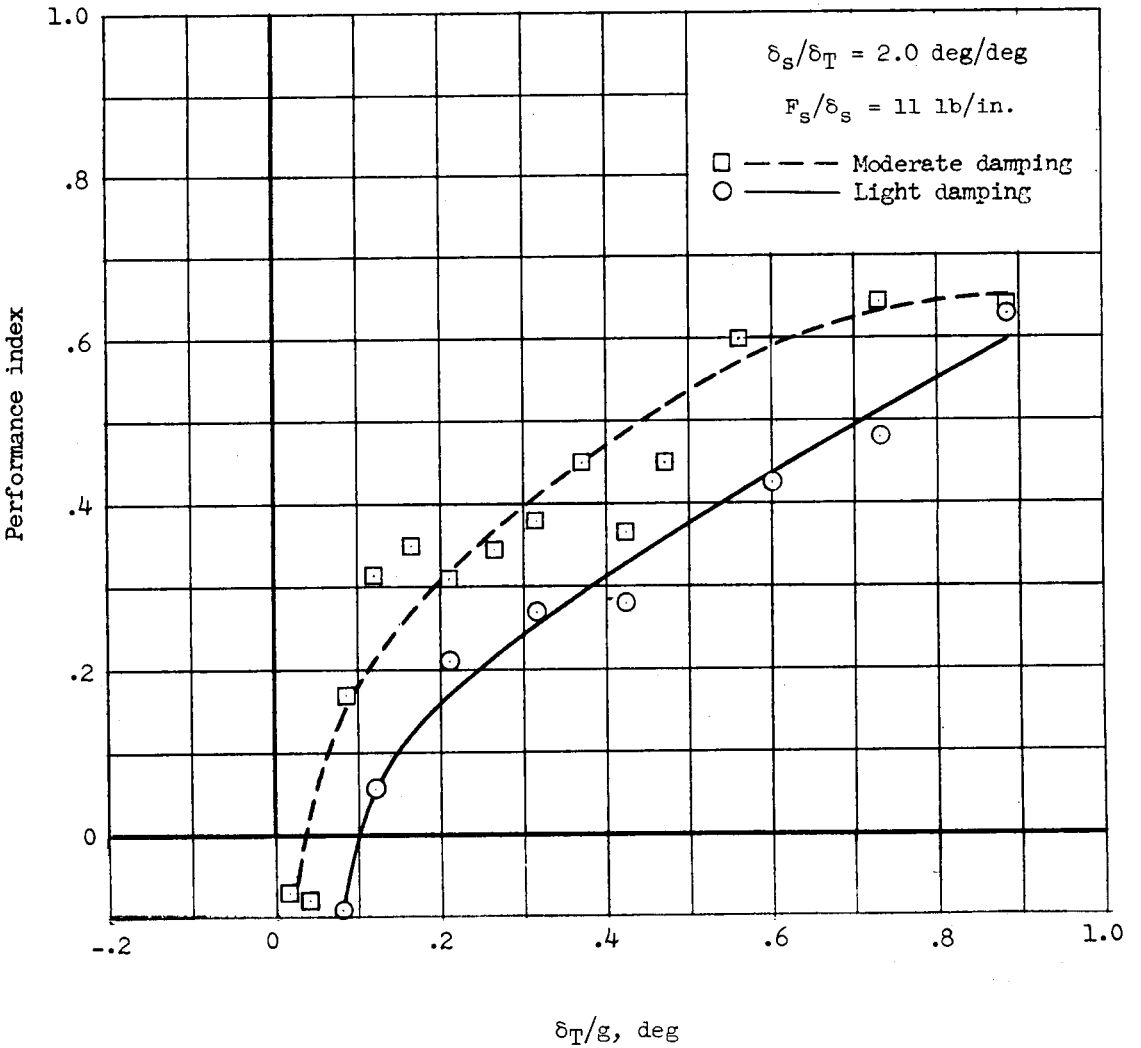

Figure 16.- Performance of pilot A through the stability range with two amounts of physical damping.

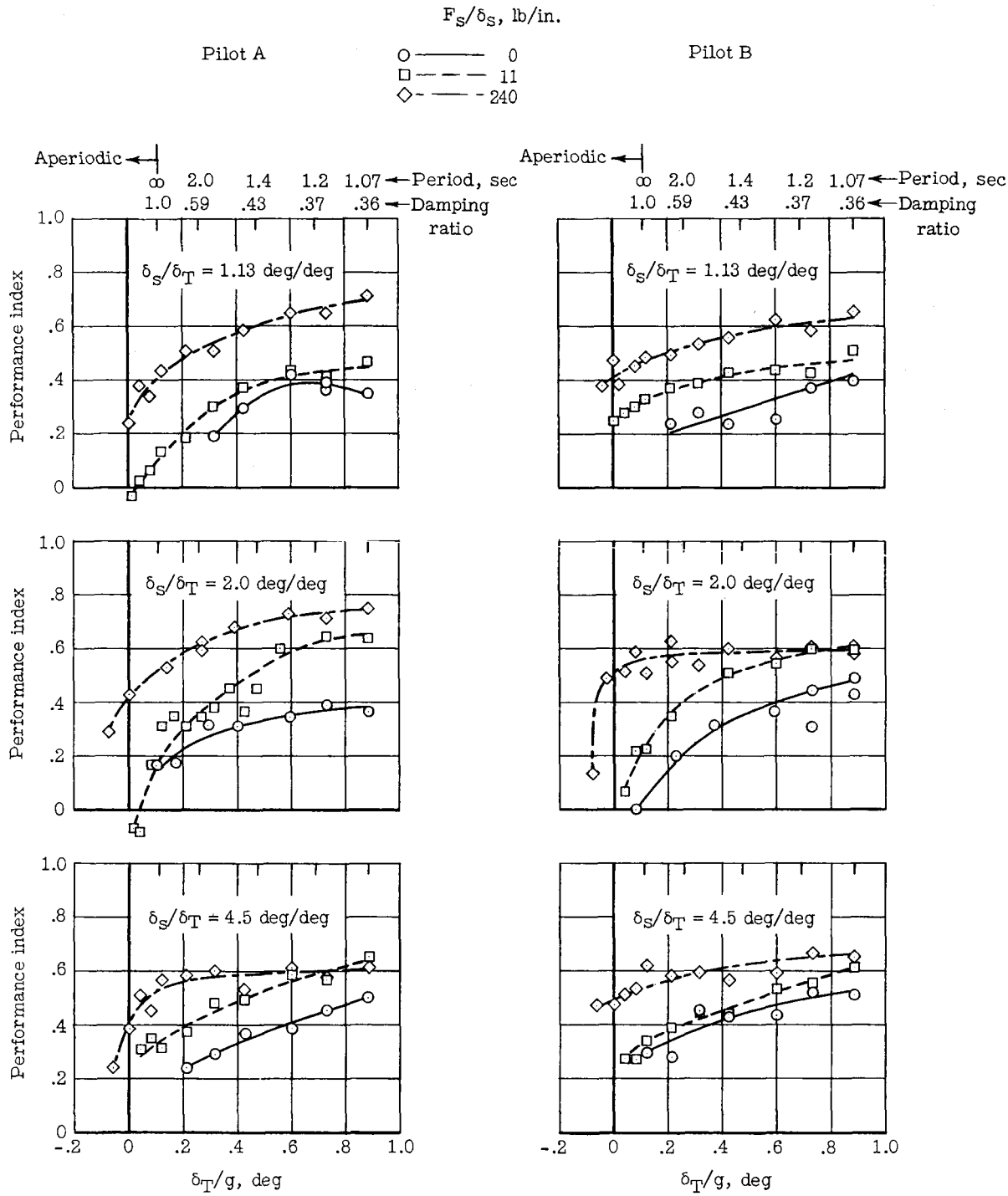

Figure 17.- Performances of both pilots throughout the stability range with various force gradients and control-system gearings.

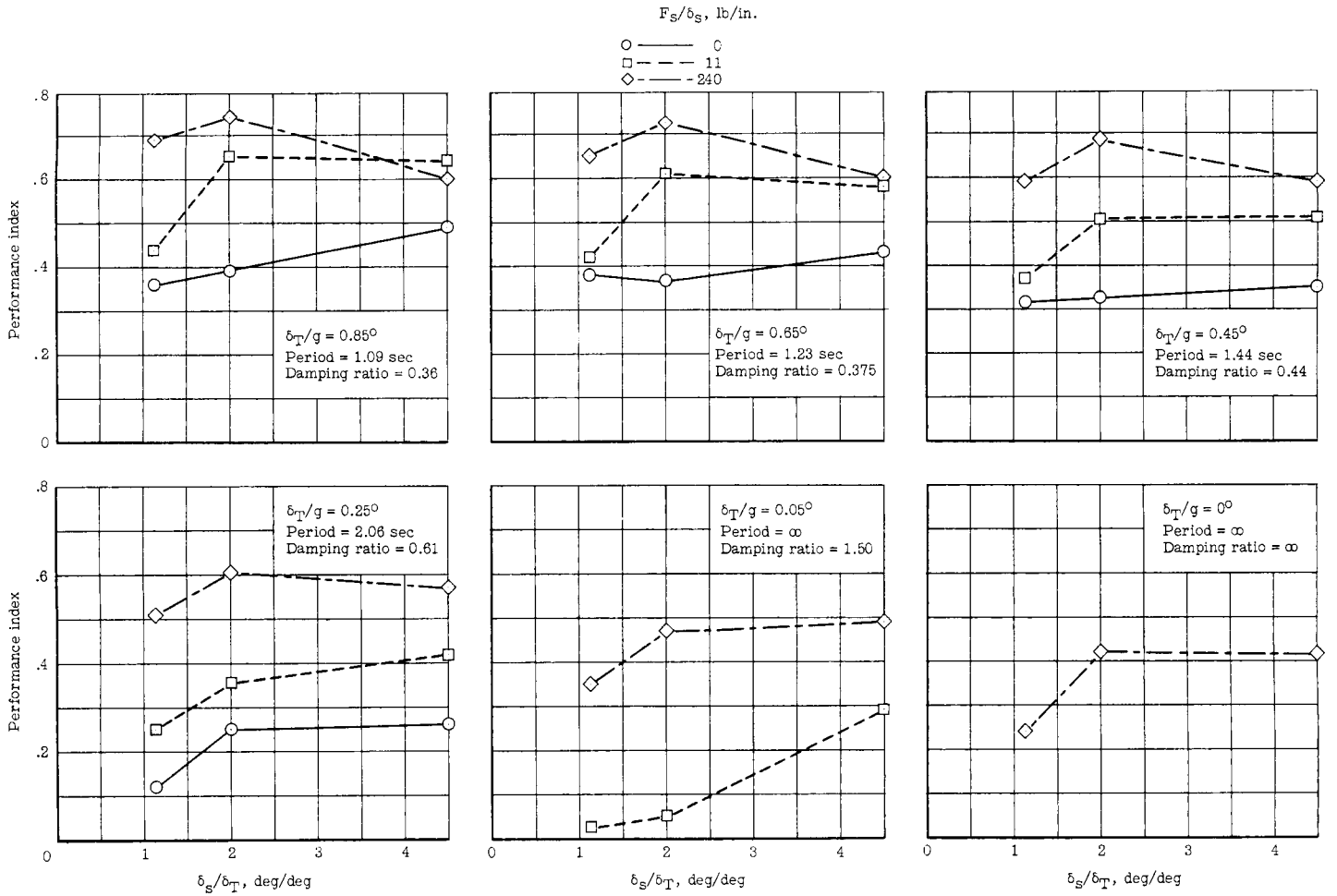

(a) Pilot A.

Figure 18.- Variation of performance with control-system gearing for three values of force gradient and various given amounts of stability.

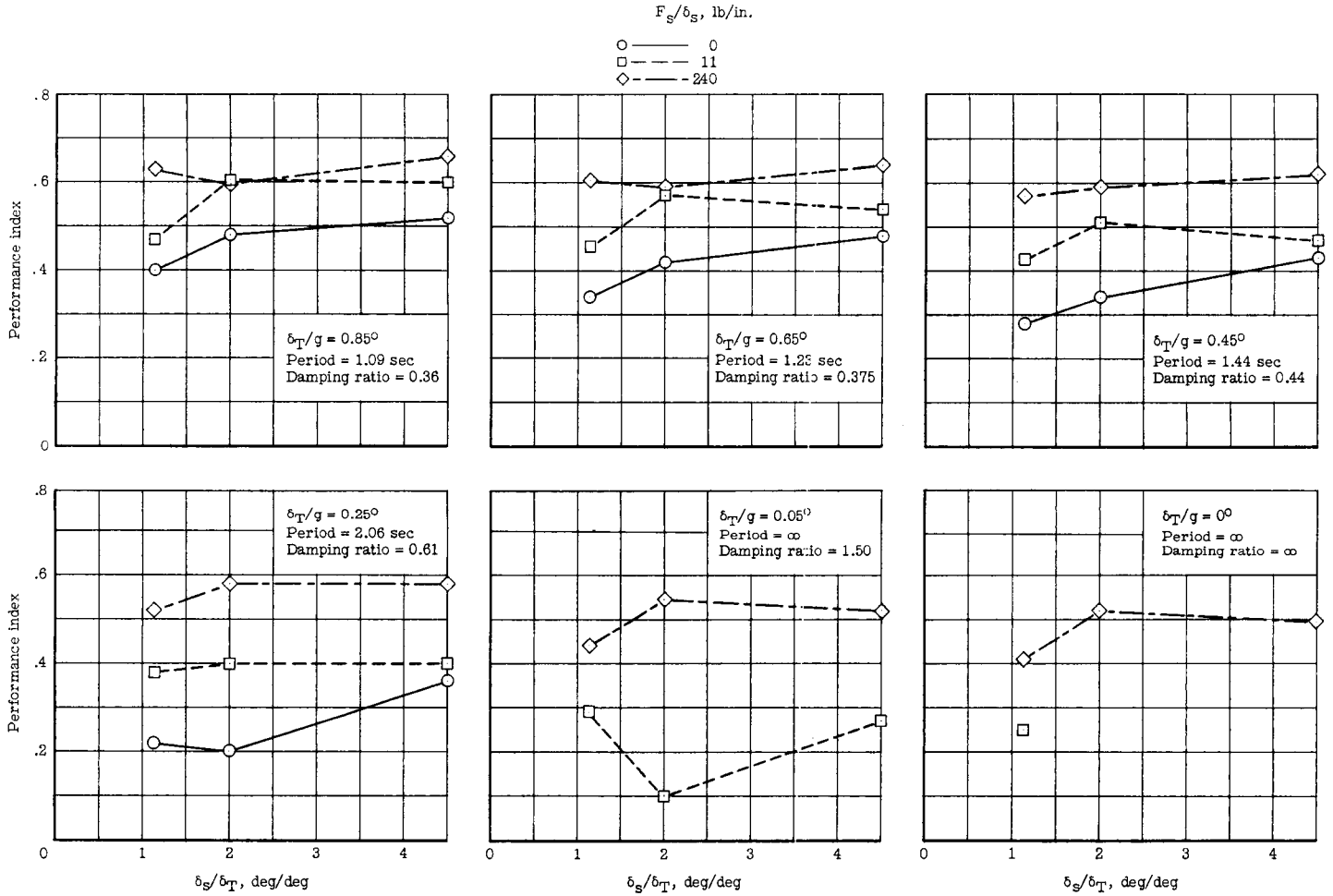

(b) Pilot B.

Figure 18.- Concluded.

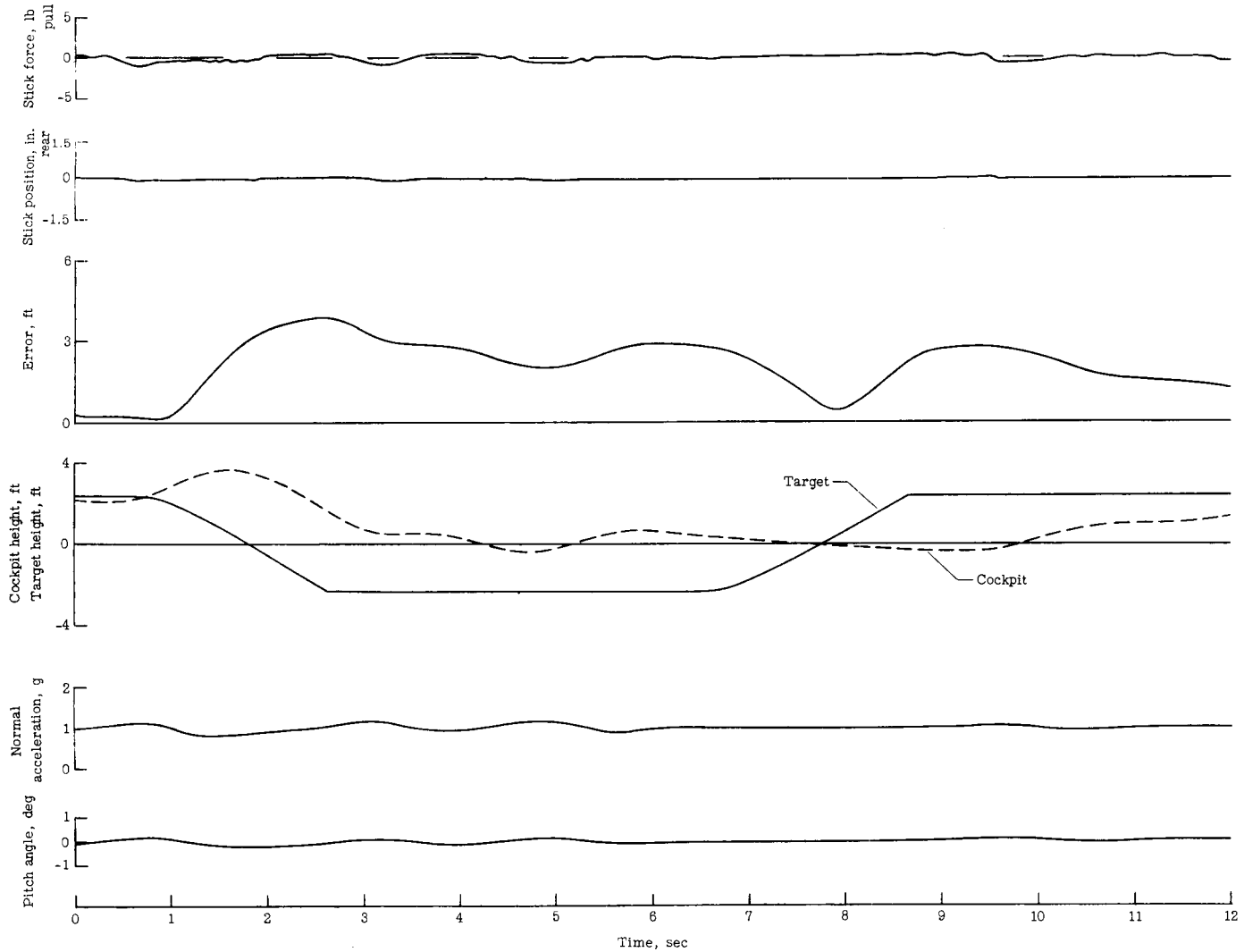

Figure 19.- Time histories of typical run with a very small amount of stability. F_s/δ_s = 11 lb/in.; δ_s/δ_T = 2.0 deg/deg; δ_T/g = 0.1; damping ratio = 1.06.

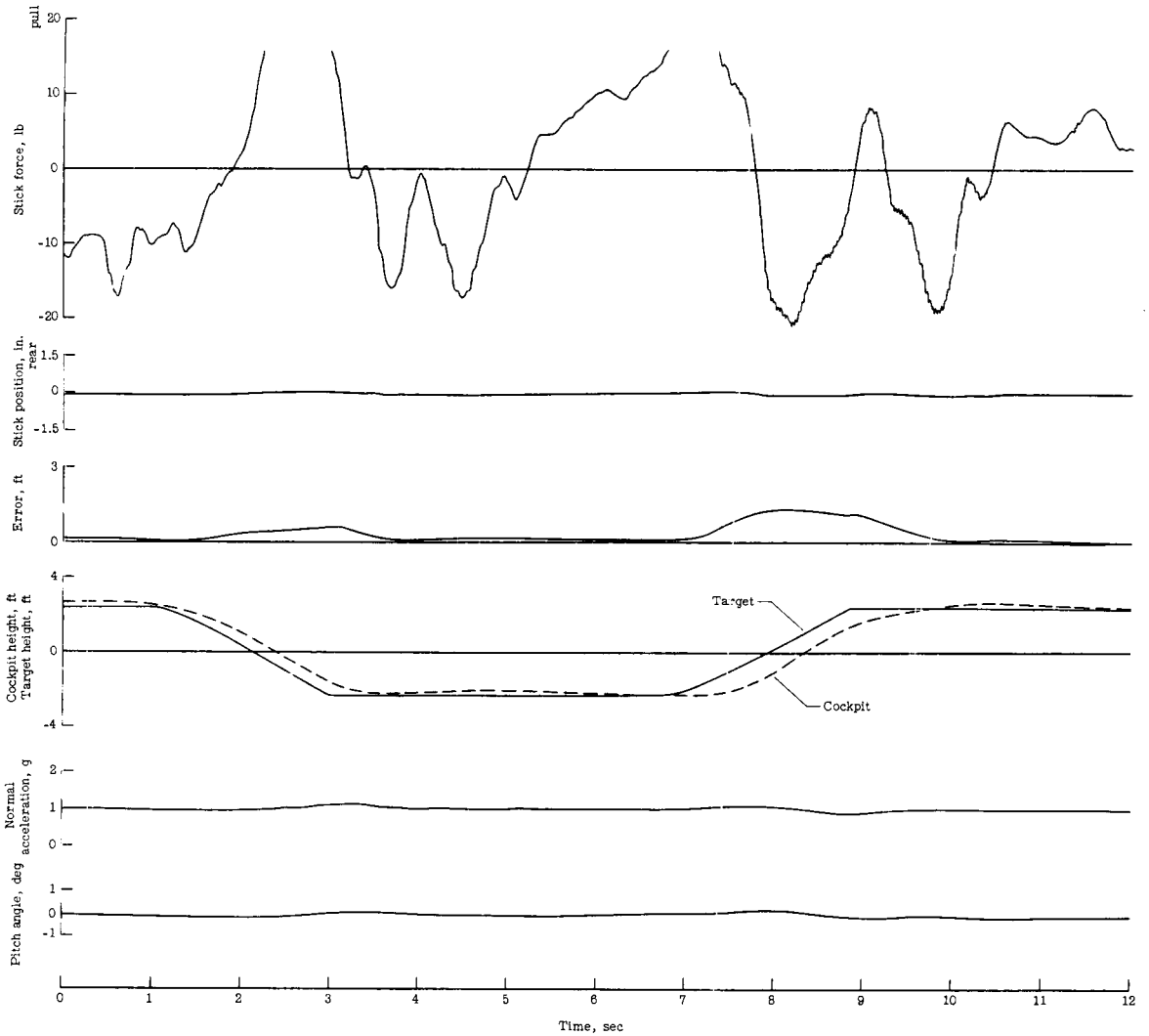

Figure 20.- Time histories of typical run with a very small amount of stability. F_s/δ_s = 240 lb/in.; δ_s/δ_T = 2.0 deg/deg; δ_T/g = 0.1; damping ratio = 1.06.

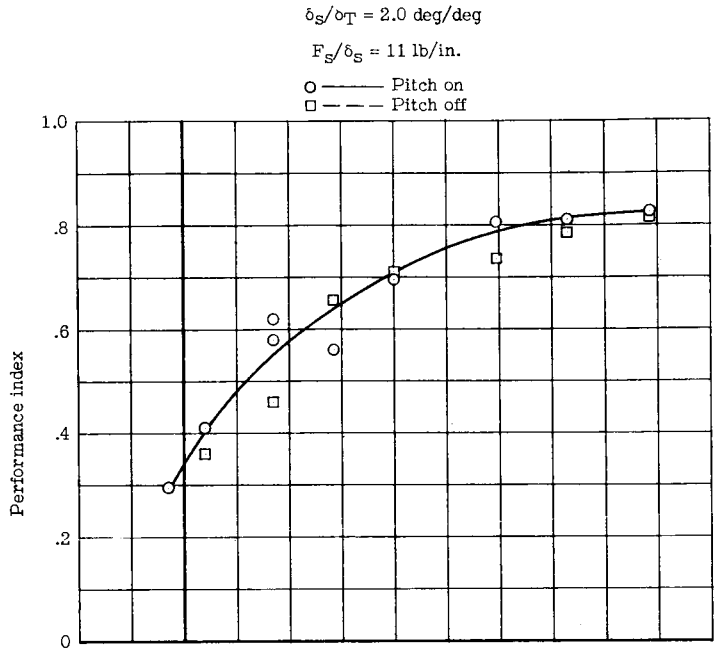

(a) Pilot A.

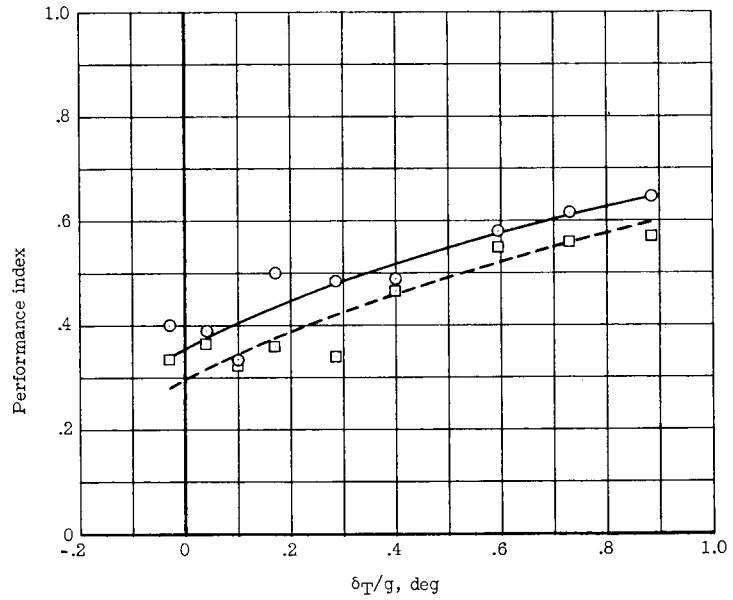

(b) Pilot B.

Figure 21.- Effect of pitching motion on performance throughout the stability range.

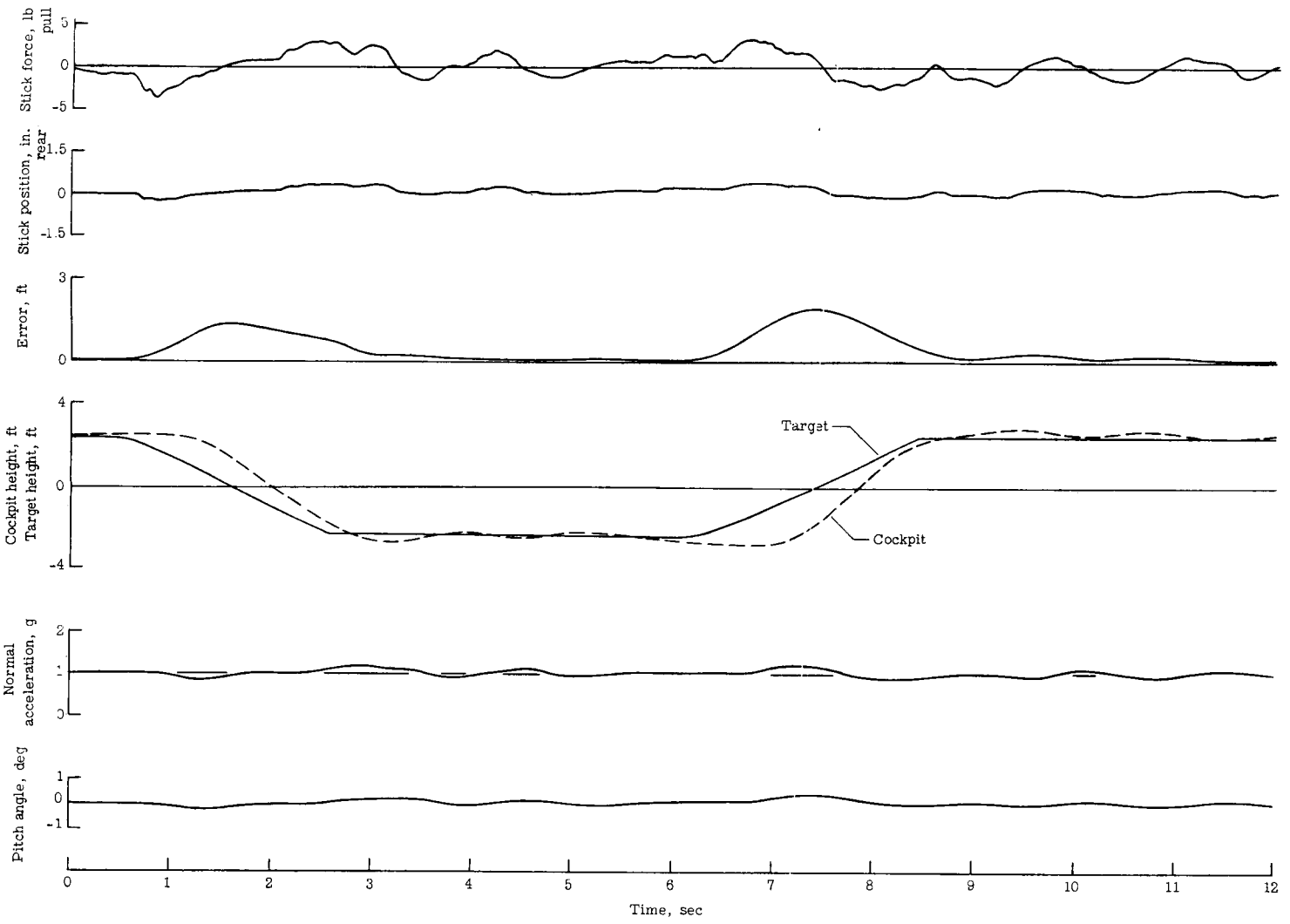

Figure 22.- Time histories of typical run with pilot A using a "desperation" type control technique. F_s/δ_s = 11 lb/in.; δ_s/δ_T = 2.0; δ_T/g = 0.89; damping ratio = 0.36.

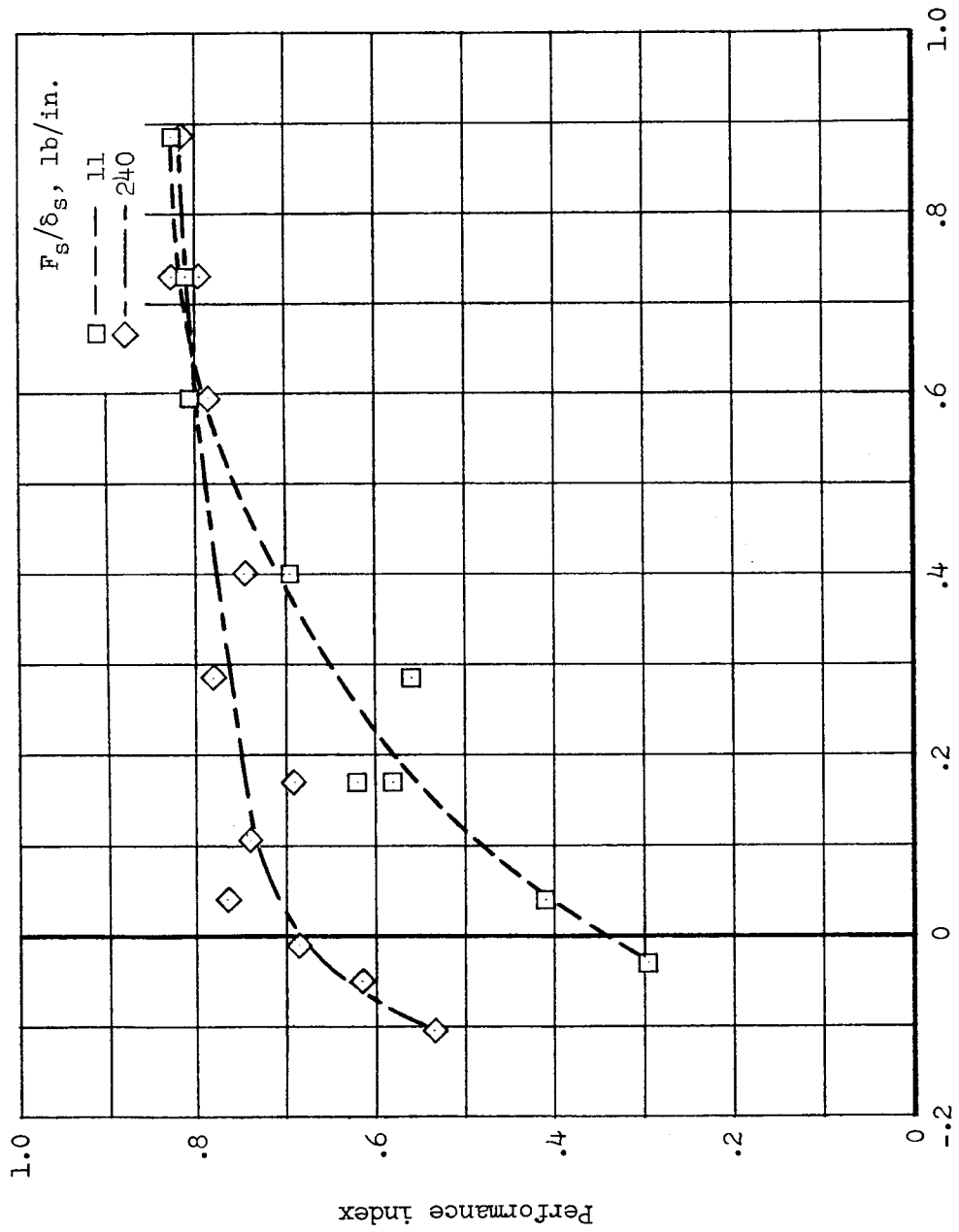

Figure 23.- Effect of force gradient on performance with pilot A using the "desperation" technique.

L-405